British Journal of Bio-Medical Research Vol.05, Issue 04, Pg.1749 - 1780, July - August 2021

Available Online at http://www.bjbmr.org

BRITISH JOURNAL OF BIO-MEDICAL RESEARCH

Cross Ref DOI: https://doi.org/10.24942/bjbmr.2021.845 Volume 05, Issue 04, July - August 2021

ISSN:2456-9739

Research Article

Complementarity Of Differential Scanning Calorimetry-Measured (DSC) Enthalpy Changes With The Hansen Solubility Parameters In Silico Prediction For Miscibility And Eutectic Screening For The Gsk-3β Inhibitor, Tideglusib And 27 Coformer Candidates

Bernard Kiernan* [a,b], Sriramakamal Jonnalagadda [a], Mike Snape [b]

[a] Philadelphia College of Pharmacy, University of Sciences, Philadelphia, PA, USA
[b] AMO Pharma Ltd, Godalming, Surrey, GU7 1RE, UK.

ARTICLE INFO

Article History:
Received on 04th July 2021
Peer Reviewed on 19th July 2021
Revised on 24th August 2021
Published on 29th August 2021

Keywords:
Calorimetry, In Silico, Hansen Solubility Parameters, eutectic screening tool

ABSTRACT

Achieving miscibility or eutectic formation for a drug substance may result in improved biorelevant physicochemical properties. The complementarity of Hansen Solubility Parameters (HSP) as a miscibility and eutectic prediction tool, with empirically-derived enthalpy of melting changes, were assessed for the GSK-3β inhibitor, tideglusib. Solubility parameters derived from both Yamamoto-molecular break ('Y-MB') and Van Krevelen methodologies were calculated. 1:1 stoichiometric mixtures of tideglusib and 27 coformer candidates were prepared by co-grinding and examined by differential scanning calorimetry. Qualitative, quantitative, and statistical assessments of the resulting endotherms and associated enthalpy changes, were performed. DSC-detected enthalpy changes were converted to a binary miscibility and eutectic scoring system which enabled logistical regression. While a greater correlation was found between Y-MB derived parameters and miscibility, statistically significant relationships exist between eutectic formation and solubility parameters derived from Y-MB methodologies i.e., δ(δTotal), Δδ-Y-MB, Ra(v)-Y-MB, hydrogen bond/donor/acceptor (δ(δH), δ(δHD), δ(δHA), and Van Krevelen methology i.e., Ra(v), Δδ. Despite the small data set and limitations, overall predicted vs. actual success rates are high, agreeing with prior literature and support the use of HSP as a miscibility and eutectic screening tool.

Corresponding Author: *Bernard Kiernan, Philadelphia College of Pharmacy, University of Sciences, Philadelphia, PA, USA.*

INTRODUCTION

Tideglusib physicochemical properties and consideration for bioavailability

Tideglusib (Figure 1), is a 1,2,4-TDZD derivative small molecule drug, (4-benzyl-2-naphthalen-1-yl-1,2,4- thiadiazolidine-3,5-dione, CAS: 865854-05-3).

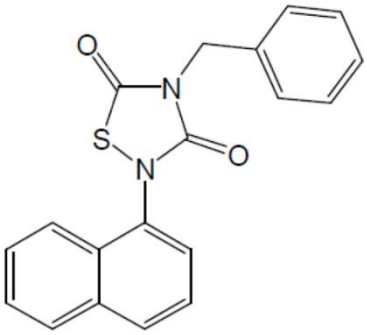

Figure 1 Tideglusib molecular structure

This drug is in clinical development for the rare disease indication of myotonic dystrophy (DM-1) (Horrigan, McMorn et al. 2018, Horrigan, Gomes et al. 2020). Previous clinical developments efforts include Autism Spectrum Disorder (Anagnostou, Bennett et al. 2018), Progressive Supranuclear Palsy (Tolosa, Litvan et al.) and Alzheimer's Disease (Lovestone, Boada et al.). The molecule demonstrates a maximum thermodynamic aqueous solubility across the physiological pH range of <0.01mg/ml (Table 1) and good permeability (logP = 4.6).

Solvent/pH	tideglusib (mg/mL)	Solubility
pH 1.2 (0.1 N HCl)	<0.01	Practically insoluble
pH 4.5 (sodium acetate buffer)	<0.01	Practically insoluble
pH 6.8 (Potassium phosphate buffer)	<0.01	Practically insoluble
Water (pH 5.6)	<0.01	Practically insoluble
Methanol	< 10	Slightly soluble
Acetonitrile	10	Sparingly soluble
Acetone	20 – 30	Soluble
DMSO	> 10	Soluble

Table 1. Tideglusib Solubility Profile

Assuming passive absorption and no site of absorption differences, and without any ionizable group on the molecule, permeability should be pH-independent throughout the gastrointestinal tract. The oral absorption of high permeability/low solubility (BCS class II) drugs (Amidon, Lennernäs et al. 1995) can be limited by poor solubility where low or variable bioavailability results. Despite a high dose number (low aqueous solubility, 1000mg QD dose), bioavailability is achieved because kinetic solubility in physiologically relevant media and consequently solubility *in vivo*, are clearly greater. This is consistent with Lipinksi's estimates for the true mininum solubility requirements as a function of permeability and dose (Lipinski 2000) (Lipinski 2003). However, low aqueous solubility/high permeability profile drugs may demonstrate positive food effects (Raman and Polli 2016) (Gu, Li et al. 2007). While food effects may be addressed at the formulation

stage by addressing solubility and/or dissolution properties or e.g., by formulating a stabilized lipophilic phase using emulsifying surfactant systems (Charman, Charman et al. 1992, Charman, Porter et al. 1997, Holm, Porter et al. 2003) this may also be addressed through the physicochemical properties of APIs via polymorphs, salts, solvates, and now, with increasing frequency, via co-crystal (Karagianni, Malamatari et al. 2018) or eutectic formation (Araya-Sibaja, Vega-Baudrit et al. 2019). Eutectics, in particular, were of interest to the authors.

Eutectics can form when two crystalline solids display miscibility in the liquid state but immiscibility in the solid state. Eutectics display a single melting peak at a lower temperature than the individual components. They typically form in non-stoichiometric ratios although some exceptions exists e.g.,hesperitin with theophylline, theobromine, gallic acid and adenine (Chadha, Karan et al. 2017). This is one of several distinguishing differences from co-crystals. While co-crystal formation is considered an enthalpy gain rather than entropy loss, eutectics are understood to form when entropy gain outweighs enthalpy loss. This is intuitive from the Gibbs free energy's temperature-entropy contribution with miscibility at molten state overcoming positive enthalpic factors. Despite dfferences, the same interactions can potentially be involved in the formation of either, at least initially. Learnings from co-crystal formation should therefore be considered for applicability.

Interactions are noncovalent and hydrogen bonding, van der Waals forces, and π-π interactions can be involved. Since components recrystallize separately into their respective crystal habits, the diffraction patterns resemble the individual components.With eutectics, there is therefore disruption in long range but not short range crystallinity. Nevertheless, this interruption may afford changes in solubility or dissolution properties, as recently reported for eutectics of lovastatin with benzoic acid, salicylic acid and cinnamic acid, with 4-5x increases in solubility (Araya-Sibaja, Vega-Baudrit et al. 2019). Similarly, Cherukuvada and Row, suggest that eutectics are designable systems that can modify the physicochemical properties of the drug (Cherukuvada and Guru Row 2014). This was yet further exemplified by Chadha, Karan et al, when attempting co-crystal formation for hesperitin, they yielded only eutectics but still achieve enhanced dissolution resulting in improvemed bioavilability (Chadha, Karan et al. 2017).

In terms of hydrogen bonding, tideglusib lacks a strong reciproating hydrogen bonding functional group such as a carboxylic acid or amide. As a di-one, it may still participate as hydrogen bond acceptors through the carbonyl oxygens. From single crystal x-ray diffraction studies (not reported here), chalcogen (S…O) interactions from the heterocycle were discovered to be the primary stabilizing force for the tideglusib crystal structure resulting in a single polymorphic form with sharp crystallinity (melting onset: 152.2°C, melting peak: 152.7°C, enthalpy: 110.3J/g). Literature also informs of the importance of non-hydrogen bonding contributions to such binary interactions such as π-π bond stacking and interactions, as exemplified by Bora, Saikia et al for cocrystals of acridine (nitrgoen substituted heteroarene), with all possible isomeric forms of dihydroxy-benzoic acid (Bora, Saikia et al. 2018). Weak interactions between aliphatic hydrogens and electronegative atoms like Oxygen (C-H..O) can be found (Dai, Voronin et al. 2019). Therefore, several forms of interaction other than a reciprocal hydrogen bonding are possible but require a tailored molecule-specific approach. Co-miscibility of tideglusib and a coformer in the molten state was considered an expected condition of eutectic formation. This concept of miscibility was explored in the work of Mohammad et al. (Mohammad, Alhalaweh et al. 2011) who noted the association between co-crystal formation and eutectics and referenced the work of Lu et al. (Lu, Rodríguez-Hornedo et al. 2008) who reported on the speed and utility of DSC to detect cocrystal and eutectic formation. Lu et al, with reference to

Nehm et al. (Nehm, Rodríguez-Spong et al. 2006), discussed cocrystal formation from eutectics. In this work, we focused on identifying miscibility interactions, including eutectic formation, as the goal. The instrumentation selected was differential scanning calorimetry (DSC).

Empirical Determination by DSC

The role of DSC in screening as either a single method or a supplemental confirmatory technique is well-documented in the literature (Lu, Rodríguez-Hornedo et al. 2008) (Saganowska and Wesolowski 2018) (Mohammad, Alhalaweh et al. 2011) (Araya-Sibaja, Vega-Baudrit et al. 2019) (Chadha, Karan et al. 2017) (Cherukuvada and Guru Row 2014). This instrument can detect both first and second order transitions and quantitative characterization of the endotherm and changes in melting onset, melting point, and enthalpy of melting can be measured. Evidence of binary system interactions from melting point depression to more significant observations of eutectic formation are possible. In this way, an empirically derived qualitative and quantitative assessment of tideglusib interaction with each of the coformer candidates can be measured.

Hansen Solubility Parameters (HSP) as an *In Silico* screening tool

Hansen Solubility Parameters were developed by Charles Hansen (Hansen 1967) with widespread application across many industries. The parameters expanded upon the earlier work of Hildebrand & Scott, that used measurements of dispersive forces (Van der Waal forces – Keesom, Debye, London depending on the permanency or induced dipole). This work resulted in the Hildebrand solubility parameter that was derived as the square root of the cohesive energy density, where the CED is defined as the heat of vaporization divided by the molar volume (Joel H. Hildebrand 1950). From Hildebrand's earlier work, the addition of polar forces and hydrogen bonding forces could expand the calculations from less complex molecules such as hydrocarbons (where dispersive forces primarily accounted for the cohesive energy density and consequently where the Hildebrand solubility parameter predicted well) to any molecular structure such as those with more polar functional groups.

HSP was previously reported for its applicability as a tool for co-crystal candidate selection (Mohammad, Alhalaweh et al. 2011) and for its reliability and inclusion/exclusion criteria in co-crystal screening tool (Nagy, Pál et al. 2019). Both papers provide comprehensive overviews of the fundamentals of the parameters and the underlying factors. Generally speaking, Hansen Solubility Parameters (HSP) can be used as a predictor of miscibility. The solubility parameter can be considered a point in 3-D space based on dispersive, polar and hydrogen forces, with an interacting distance or radius. Alternatively, the parameter may be considered uni-dimensional. Small differences suggest high probability of miscibility while larger differences predict immisciblity. As described by Mohammad et al., throughout literature, there are multiple expressions for solubility parameter differences (Krevelen 2009) (Bagley, Nelson et al. 1971) (Greenhalgh, Williams et al. 1999). Van Krevelen, using their method of force estimations for dispersive, polar and hydrogen bonding defined the term, $\Delta\delta$, which is simply the distance between two points in 3D space. It was noted by Van Krevelen that their estimations of parameters were of the same order of accuracy as that of Hoy (Hoy 1985) and therefore for estimation, both methods were applied and results averaged. For polymer/solvent combinations good solubility occurs if $\Delta\delta \leq 5$ $Mpa^{1/2}$and this can be applied for miscibility of two solids. Bagley et al. developed the radius of interaction and miscibility is expected where $Ra(v) < 5.6$ $MPa^{1/2}$ and proposed a two-dimensional Bagley diagram that plots an expression for dispersion and polar forces as a single value ('δv') vs hydrogen bonding force ('δH') to express the three variables of dispersion, polar, and hydrogen bonding in two-dimensional cartesian plots. Another term 'δa' had earlier summarized polar and hydrogen bonding forces together per the work of Hansen who proposed

that dispersion forces could be approximated to a simple hydrocarbon of the same general structure. By subtracting this estimate for dispersive forces from the total solubility parameter, the difference was therefore equal to the sum of the remaining polar and hydrogen bonding forces.

Mohammad et al.'s findings correlated well with assumptions on HSP distances but did uncover exceptions otherwise not predicted by the Δδ and Ra(v) parameters. In fact, there was closer correlation using simply the absolute difference between values, citing Greenhalgh et al.'s work (Greenhalgh, Williams et al. 1999) that was also surprising since Greenhalgh et al. only calculated dispersive forces, per Hildebrand solubility parameters, excluding polar and hydrogen bonding forces.

It is therefore clear that adherence to literature recommendations for HSP distances for miscibility/immiscibility, using only a single expression, can clearly present a risk of excluding viable candidates. To further reinforce this point, the work of Nagy et al. (Nagy, Pál et al. 2019) sought to revisit the reliability of HSP for cocrystal prediction and to revisit the inclusion cut-off values (i.e. HSP distances) by the various expressions. Their work recommended continued adherence to Greenhalgh et al. distances since their findings (8.18 $MPa^{1/2}$) were within ~1 $MPa^{1/2}$ of the previously suggested 7 $MPa^{1/2}$ cut-off. However, they recommended widening Δδ and Ra(v) distances i.e. those of (Van Krevelen and Te Nijenhuis 1990) and (Bagley, Nelson et al. 1971), to 16.87 $MPa^{1/2}$ and 17.64 $MPa^{1/2}$, respectively. The applicability of these cut-off values was of interest in this study.

To reiterate, this work considers miscibility and not cocrystal formation to be the target, consistent with the original intent and power of the HSP. The work assesses the complementarity of *in silico* predictive modelling and empirical calorimatric methods towards the identification of miscible coformer candidates. Statistical relationships can be investigated for these expressions and individual dispersive vs. polar vs. hydrogen bonding forces for all binary systems as independent variables against enthalpy of melting changes. In this way both summary values and categorical forces e.g. dispersive (π-π interaction/stacking) vs. hydrogen bonding, may be examined.

Experimental

Hansen Solubility Parameters in Practice (HSPiP) software was used.

In Silico Hansen Solubility Parameters

Calculation using Y-MB, δ(δTotal)

The Hansen Solubility Parameters δD, δP, and δH, were calculated for tideglusib and 71 coformer candidates, using the software's Yamamoto-Molecular Break ('Y-MB') application (a group contribution method) through the submission of SMILES structures for each coformer of interest. Values are tabulated (**Table 2**) for dispersive, polar, and hydrogen-bonding forces, and by HSP difference 'δ(δTotal)' (**Equation 1**). Estimates for hydrogen bond acceptance and hydrogen bond donor characters are also presented in **Table 2**. These are the contributions of hydrogen bond donor and acceptor character to overall δH.

δ(δTotal):

$$\delta(\delta Total) = (\delta Total_{tide} - \delta Total_{coformer}), \text{ where } \delta Total = [(\delta D)^2 + (\delta P)^2 + (\delta H)^2]^{1/2} \quad \textbf{Equation 1}$$

Qualitative Coformer Selection

The pool of 71 potential candidates was generated from internal resources and from literature (Schultheiss and Newman 2009) (Panzade, Shendarkar et al. 2017) (Mohammad, Alhalaweh et al. 2011). For practical consideration, a subset of 27 coformers was selected. A practical qualitative approach to ensuring a representative sample considered the individual solubility parameters, the value of δ(δTotal) and the hydrogen bond donor and acceptor character. The 27 coformers that were

selected spanned the full spectrum of 'HSP distance' using 'δ(δTotal)' to quantify this distance (Equation 1). It was previously reported that for solubility, δ(δTotal) <5 $MPa^{1/2}$. Coformers were therefore selected ensuring a reasonable distribution across three categories: δ(δTotal) <5 $Mpa^{1/2}$, 5$Mpa^{1/2}$ < δ(δTotal) <10 $MPa^{1/2}$, δ(δTotal) > 10 $MPa^{1/2}$ including 7 coformers with large δ(δTotal) values as 'controls' for expected non-interaction. The distribution of δ(δTotal) distances for the pool and selected is presented in **Figure 2**.

The 3-D design space for the selected coformers, pool and the reference point (tideglusib, δD=20.50, δP=4.70, δH: 5.00) is presented in **Figure 3 (A)**. A plot of hydrogen bond acceptance character **δH A** vs. hydrogen bond donor character **δH D** is also presented in **Figure 3 (B).**

Coformer	δD	δP	δH	δTotal	δ(δTotal)	δH D	δ(δH D)	δH A	δ(δH A)
Tideglusib	***20.5***	***4.7***	***5***	***21.62***	***0***	***0.1***	***0***	***4.4***	***0***
1,2 dihydroxybenzene	***18.8***	***8***	***15.9***	***25.74***	***-4.13***	***13***	***-12.9***	***8.9***	***-4.5***
1-hydroxy-2-napthoic acid	***20.4***	***5.2***	***14.1***	***25.34***	***-3.72***	***9.8***	***-9.7***	***9.4***	***-5***
2-methoxy benzoic acid	19.3	7.5	10	22.99	-1.38	7.6	-7.5	6.8	-2.4
2-Picolinamide	19.9	15.1	12.8	28.07	-6.45	7.5	-7.4	9.6	-5.2
3,4-Dihydroxybenzoic acid	20.6	9.5	18.8	29.46	-7.84	15.9	-15.8	10.5	-6.1
4-Methoxybenzoic acid	19.4	7.9	10.5	23.43	-1.81	7.8	-7.7	7	-2.6
5-Methylfurfurylamine	17.9	6	8	20.5	1.11	3.7	-3.6	6.7	-2.3
Adenine	21.3	16.4	15.6	31.08	-9.46	11	-10.9	9.3	-4.9
adipic acid	***17***	***8.5***	***17.7***	***25.97***	***-4.35***	***14.7***	***-14.6***	***10.2***	***-5.8***
anthranilic acid	***20.2***	***8.1***	***14.1***	***25.93***	***-4.31***	***10.1***	***-10***	***8.8***	***-4.4***
Ascorbic acid	20.3	14.2	25.8	35.77	-14.15	19.9	-19.8	20.5	-16.1
benzoic acid	***19.2***	***6.3***	***10***	***22.55***	***-0.93***	***8.5***	***-8.4***	***6.5***	***-2.1***
Caffeine	***19.6***	***12.5***	***8.5***	***24.75***	***-3.13***	***6.6***	***-6.5***	***7.1***	***-2.7***
Caprolactam	18.3	12.5	7.1	23.27	-1.65	4.6	-4.5	5	-0.6
cinnamic acid	***19***	***5.4***	***11.3***	***22.78***	***-1.14***	***8.7***	***-8.6***	***7.3***	***-2.9***
Citric Acid	***17.6***	***11.4***	***26***	***33.4***	***-11.76***	***22.3***	***-22.2***	***15.3***	***-10.9***
Cytosine	20.1	15.6	11.7	28	-6.39	11.7	-11.6	5	-0.6
D,L-Aspartic acid	17.1	10.6	23.1	30.63	-9.01	16.5	-16.4	14	-9.6
D,L-Mandelic acid	19.2	7.9	17.8	27.35	-5.73	13.5	-13.4	11.7	-7.3
D,L-Phenylalanine	18.5	6	12.5	23.12	-1.5	9	-8.9	8.2	-3.8
D-Glucuronic acid	16.8	12.7	23.5	31.56	-9.94	20.8	-20.7	19.2	-14.8
E,E-Sorbic acid	17.7	6.2	12.7	22.65	-1.03	9.9	-9.8	7.8	-3.4
ferulic acid	***19.8***	***7.6***	***15.8***	***26.45***	***-4.83***	***12.4***	***-12.3***	***9.1***	***-4.7***
Formamide	17.7	21.5	20.5	34.58	-12.96	16.2	-16.1	14.1	-9.7
Formic acid	14.2	8.6	13.3	21.27	0.35	11.2	-11.1	9.7	-5.3
Fumaric acid	***18.2***	***10.8***	***23***	***31.26***	***-9.64***	***18.8***	***-18.7***	***13.2***	***-8.8***
Gallic Acid	***21***	***9.8***	***18.8***	***29.84***	***-8.22***	***19.8***	***-19.8***	***9.1***	***-4.7***
glutaric acid	***17.1***	***9.7***	***19.7***	***27.63***	***-8.21***	***16***	***-15.9***	***11.4***	***-7***
Glycine	17	10.8	20	28.38	-6.77	13.8	-13.7	13.9	-9.5
hippuric acid	***19.6***	***12.8***	***14.4***	***27.48***	***-5.87***	***11.6***	***-11.5***	***9.3***	***-4.9***
Imidazole	19.7	12.5	12	26.24	-4.62	10.6	-10.5	8.1	-3.7
Lactose	16.9	11.2	19	27.79	-6.17	32.1	-32	15.1	-10.7
L-Alanine	16.8	8.8	18	26.15	-4.53	12.7	-12.6	11.7	-7.3
L-Arginine	16.8	9.6	12.1	22.82	-1.2	7.7	-7.6	7.7	-3.3
L-Asparagine	18	15.8	21.7	32.32	-10.7	15.1	-15	13.5	-9.1
L-Cysteine	17.8	9.5	18.2	27.17	-5.55	25.4	-25.3	12.5	-8.1
L-Cystine	17.3	10.9	18.4	27.51	-5.89	10.6	-10.5	12.3	-7.9
L-Glutamic acid	17	9.7	21.7	29.22	-7.6	15	-14.9	13	-8.6
L-Glutamine	17.7	14.7	20.4	30.75	-9.13	13.7	-13.6	12.5	-8.1
L-Histidine	18.6	11.8	17	27.82	-6.21	13.2	-13.1	10.2	-5.8
L-Methionine	17.9	7.8	14.5	24.32	-2.7	9	-8.9	10.1	-5.7
L-Proline	17.8	8.7	14.5	24.55	-2.93	11.5	-11.4	8.9	-4.5
L-Pyroglutamic acid	19	13.1	15.8	27.97	-6.35	12.9	-12.8	9.4	-5
L-Serine	17.7	11.7	24.3	32.26	-10.64	16.9	-16.8	16.9	-12.5
L-Threonine	17.5	9.9	21.2	29.22	-7.6	13.4	-13.3	14	-9.6
L-Tryptophan	19.6	8.3	13	24.94	-3.32	11.2	-11.1	8.3	-3.9
L-Tyrosine	19.5	7.9	17.1	27.11	-5.49	13.4	-13.3	10.3	-5.9
Lysine	16.8	7.2	14.3	23.21	-1.59	9	-8.9	9.1	-4.7
Maleic acid	***18.2***	***10.8***	***23***	***31.26***	***-9.64***	***18.8***	***-18.7***	***13.2***	***-8.8***
Malonic Acid	***17.5***	***11.9***	***24.2***	***32.15***	***-10.53***	***19.7***	***-19.6***	***14.6***	***-10.2***
Meglumine	17.4	10.3	24.4	31.69	-10.07	14.1	-14	21.3	-16.9
Melamine	21.4	16	23.4	35.52	-13.9	14.2	-14.1	16.3	-11.9
Nicotinamide	***19.9***	***15.1***	***12.8***	***28.07***	***-6.45***	***7.5***	***-7.4***	***9.6***	***-5.2***
Nicotinic acid	***19.8***	***9.8***	***11***	***24.68***	***-3.06***	***8.7***	***-8.6***	***8.4***	***-4***
Orotic acid	20.4	18	18.5	32.9	-11.28	15.7	-15.6	10.5	-6.1
oxalic acid	***17.8***	***13.8***	***26.2***	***34.55***	***-12.93***	***22.1***	***-22***	***16.9***	***-12.5***
p-amino benzoic acid	***20.3***	***8.6***	***14.6***	***26.44***	***-4.82***	***10.2***	***-10.1***	***9***	***-4.6***
Pimelic acid	16.9	7.9	16.4	24.84	-3.22	13.6	-13.5	9.5	-5.1
Resorcinol	***19.6***	***7.7***	***16.2***	***27.63***	***-6.22***	***16***	***-15.9***	***8.1***	***-3.7***
Saccharin	***21.5***	***20.6***	***10***	***31.41***	***-9.79***	***5.9***	***-5.8***	***7.7***	***-3.3***
Stearic acid	16.2	2.8	5.2	17.24	4.38	4.1	-4	3.4	1
Suberic acid	16.8	7.4	15	23.71	-2.09	12.5	-12.4	8.9	-4.5
succinic acid	***17.3***	***10.6***	***21.8***	***29.78***	***-8.16***	***17.6***	***-17.5***	***13***	***-8.6***
Sucrose	16.8	10	18	26.58	-4.96	16.3	-16.2	20	-15.6
Tartaric acid	***17.8***	***14***	***29.2***	***36.95***	***-15.33***	***22***	***-21.9***	***19.1***	***-14.7***
Theophylline	19.7	15.4	10.5	27.12	-5.5	8.4	-8.3	5.7	-1.3
Tromethamine	18.9	11.8	26.4	34.55	-12.93	15.7	-15.6	17.9	-13.5
Urea	***19.7***	***19.6***	***21.3***	***35.13***	***-13.51***	***16.3***	***-16.2***	***16.2***	***-11.8***
Vanillic acid	***19.8***	***8.6***	***15.3***	***26.48***	***-4.84***	***11.3***	***-11.2***	***8.9***	***-4.5***
Xanthine	***21.3***	***27.4***	***19.3***	***39.71***	***-18.09***	***16.2***	***-16.1***	***9.8***	***-5.4***
Xylitol	***17.7***	***11.5***	***28.9***	***35.79***	***-14.17***	***20.1***	***-20***	***21.1***	***-16.7***

Table 2. Summary Table of Dispersive, Polar and Hydrogen Bonding Forces of the Hansen Solubility Parameters for tideglusib and coformer candidates using Y-MB

Statistical Analysis Confirmation of Coformer Selection

The validity of the subset as representative was confirmed statistically by one-way ANOVA for equivalence of mean distances, comparing the absolute difference '|δ(δTotal)|' for the subset with the remaining pool of 44 coformers. A one-way ANOVA (α = 0.05, equal variances assumed) also assessed differences in δHA and δHD. The p-values for all three analyses (p=0.130, 0.870, 0.299) failed to reject the null (null: no difference) and therefore mean distances were equivalent between samples. Confidence intervals and plots are presented in Figure 4.

In Silico Hansen Solubility Parameters Calculation using Y-MB: Δδ-Y-MB, Ra(v)–Y-MB

Solubility parameters using the HSPiP software's Y-MB methodology were also used to calculate Δδ-Y-MB distance and 'Ra(v)-Y-MB'. Δδ-Y-MB distance, the distance between two points in cartesian 3-D space, is the square root of the sum of the square differences. Van Krevelen referred to this distance as Δδ and it is denoted as Δδ-Y-MB here to distinguish it as the distance between two points δD_1, δP_1, δH_1 and δD_2, δP_2, δH_2 using Y-MB calculated parameters. Ra(v)-Y-MB refers to the radius of interaction as previously used by Bagley but again, using Y-MB derived solubility parameters instead of Van Krevelen methods. Distances based on **Equation 2** and **Equation 3**were subsequently calculated for the selected 27 coformer candidates (**Table 3**).

Δδ-Y-MB:

$$\Delta\delta\text{-Y-MB} = [(\delta D_{tide} - \delta D_{coformer})^2 + (\delta P_{tide} - \delta P_{coformer})^2 + (\delta H_{tide} - \delta H_{coformer})^2]^{1/2} \quad \textbf{Equation 2}$$

Radius of Interaction, 'Ra(v)–Y-MB':

$$\text{Ra(v)–Y-MB} = [4*(\delta V_{tide} - \delta V_{coformer})^2 + (\delta H_{tide} - \delta H_{coformer})^2]^{1/2} \quad \delta V = [(\delta D)^2 + (\delta P)^2]^{1/2} \quad \textbf{Equation 3}$$

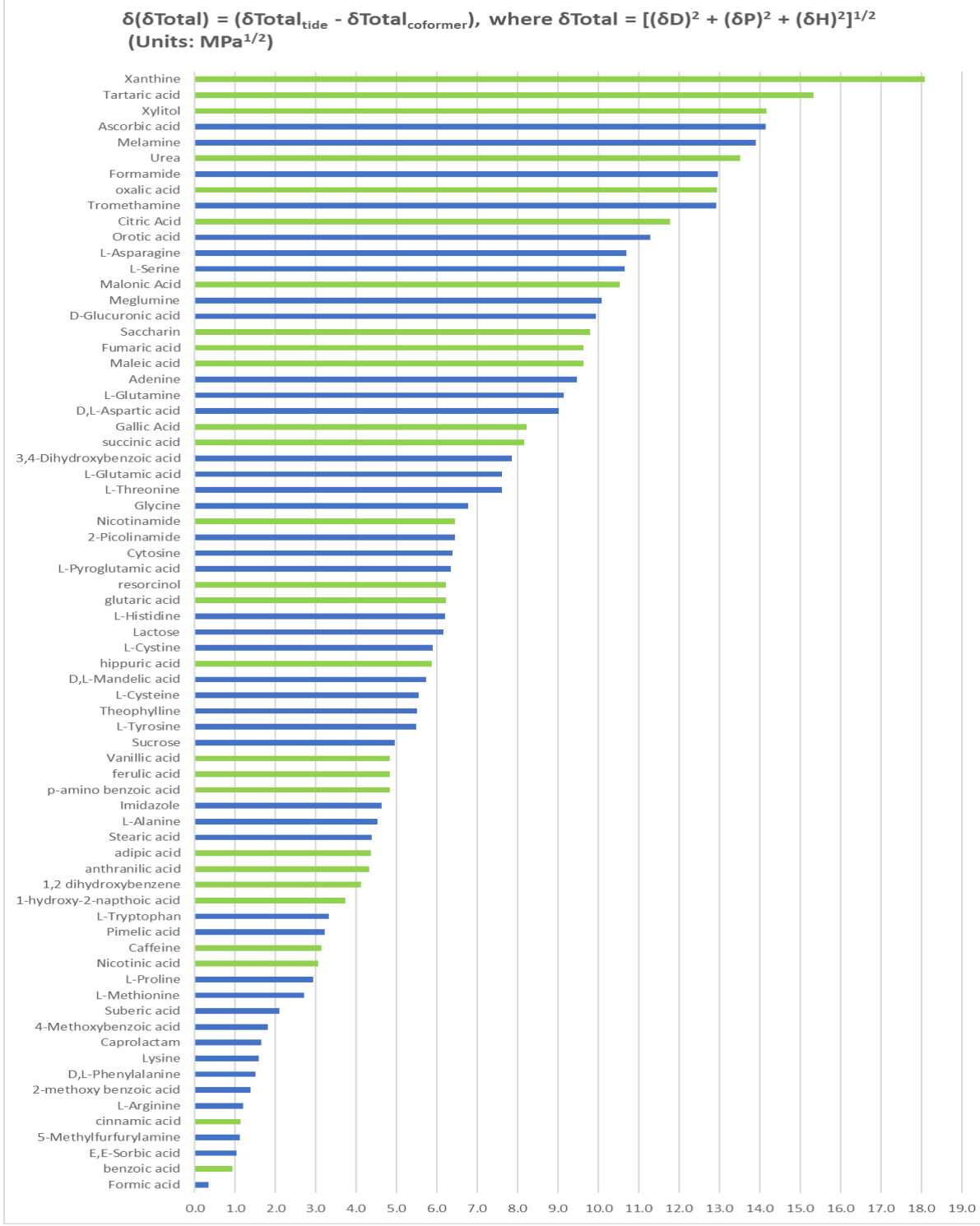

Figure 2. δ(δTotal) for tideglusib and coformer pool using Y-MB (Selected coformers denoted in green)

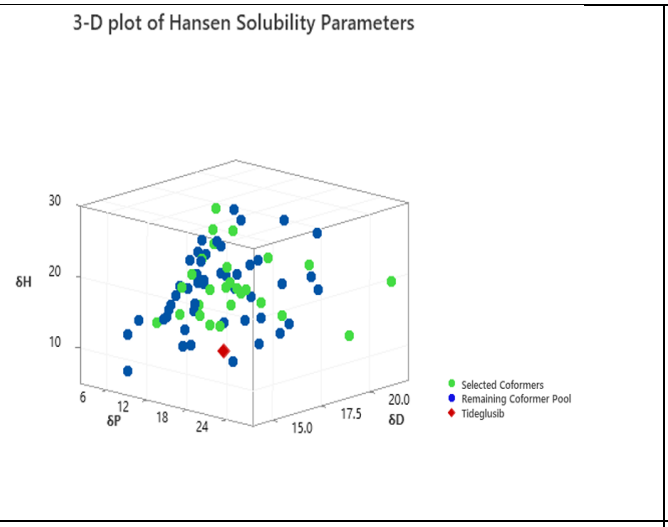

(a)

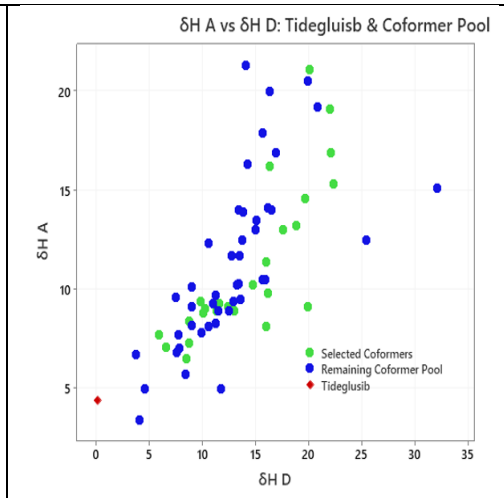

(b)

Figure 3. Design Space For Tideglusib vs. Coformer Pool Selection using Y-MB derived values: (a) δD vs δP vs δH, (b) hydrogen bonding Acceptor vs Donor

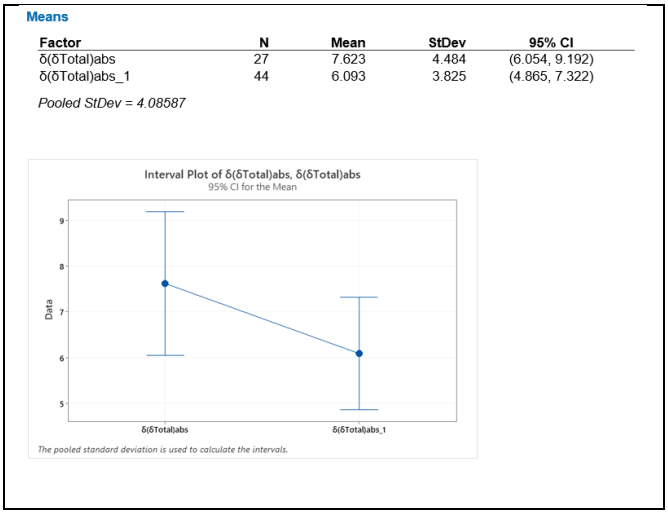

Means

Factor	N	Mean	StDev	95% CI
δ(δTotal)abs	27	7.623	4.484	(6.054, 9.192)
δ(δTotal)abs_1	44	6.093	3.825	(4.865, 7.322)

Pooled StDev = 4.08587

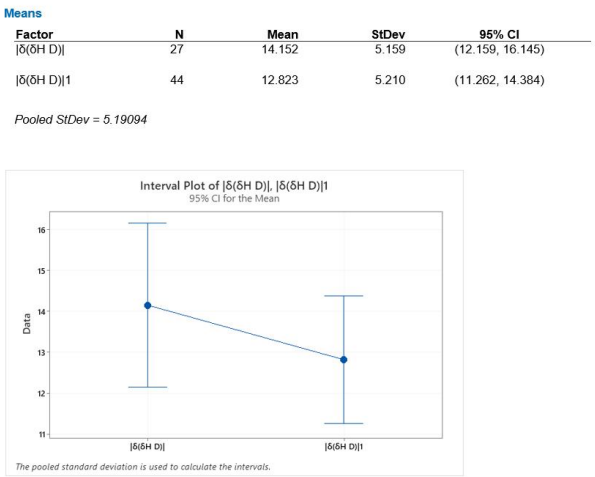

Means

Factor	N	Mean	StDev	95% CI
|δ(δH D)|	27	14.152	5.159	(12.159, 16.145)
|δ(δH D)|1	44	12.823	5.210	(11.262, 14.384)

Pooled StDev = 5.19094

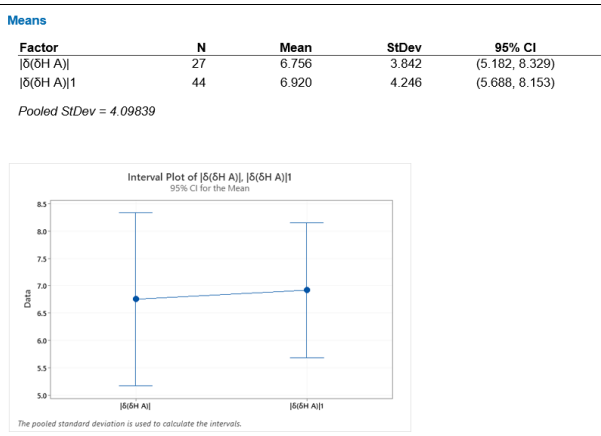

Means

Factor	N	Mean	StDev	95% CI
|δ(δH A)|	27	6.756	3.842	(5.182, 8.329)
|δ(δH A)|1	44	6.920	4.246	(5.688, 8.153)

Pooled StDev = 4.09839

Figure 4. One-Way ANOVA for coformer selection

Coformer	Δδ-Y-MB	Ra(v)-Y-MB
Tideglusib	0.00	0.00
1,2 dihydroxybenzene	11.55	11.01
1-hydroxy-2-napthoic acid	9.11	9.10
adipic acid	13.71	13.33
anthranilic acid	9.72	9.22
benzoic acid	5.41	5.27
Caffeine	8.60	5.65
cinnamic acid	6.51	6.80
Citric Acid	22.23	21.00
ferulic acid	11.20	10.81
Fumaric acid	19.14	18.00
Gallic Acid	14.72	14.45

glutaric acid	15.89	14.95
hippuric acid	12.44	10.53
Maleic acid	19.14	18.00
Malonic Acid	20.72	19.20
Nicotinamide	13.01	11.10
Nicotinic acid	7.91	6.36
oxalic acid	23.23	21.41
p-amino benzoic acid	10.36	9.81
Resorcinol	13.57	13.20
Saccharin	16.70	18.19
succinic acid	18.09	16.87
Tartaric acid	26.07	24.41
Urea	22.23	21.36
Vanillic acid	11.04	10.36
Xanthine	26.84	30.86
Xylitol	25.01	23.90

Table 3. Summary Table of the Solubility Parameter Distances Δδ-Y-MB and Ra(v)–Y-MB for tideglusib and coformer candidates using Y-MB

In Silico Hansen Solubility Parameters Calculation using Van Krevelen: Δδ, Ra(v)

Solubility parameters using the Van Krevelen methodology were also determined using HSPiP software and used to calculated Δδ and Ra(v). Distances based on Equations 4 and 5 were calculated for the coformer candidates (**Table 4**).

Δδ:

$$\Delta\delta = [(\delta D_{tide} - \delta D_{coformer})^2 + (\delta P_{tide} - \delta P_{coformer})^2 + (\delta H_{tide} - \delta H_{coformer})^2]^{1/2} \quad \textbf{Equation 4}$$

(δD , δP, δH values derived from Van Krevelen methodology)

Radius of Interaction, Ra(v):

$$Ra(v) = [4*(\delta V_{tide} - \delta V_{coformer})^2 + (\delta H_{tide} - \delta H_{coformer})^2]^{1/2} \quad \delta V = [(\delta D)^2 + (\delta P)^2]^{1/2} \quad \textbf{Equation 5}$$

(δD , δP, δH values derived from Van Krevelen methodology)

The molecular structure, molecular weight, melting points, hydrogen bond donor and acceptor counts for all 27 coformer candidates are presented in **Table 5** and **Table 6**, for aromatic and non-aromatic coformers, respectively.

Coformer	δD	δP	δH	Δδ	Ra(v)
Tideglusib	20.3	6.5	7.6	0.00	0.00
1,2 dihydroxybenzene	18.1	5.4	20.7	13.33	13.97
1-hydroxy-2-napthoic acid	17.3	4.4	14.1	7.46	9.50
adipic acid	17.1	4.8	12.6	6.17	8.69
anthranilic acid	19.5	4.1	13.1	6.05	6.16
benzoic acid	19.2	4.3	9.9	3.37	4.01
Caffeine	17	12.5	12.4	8.36	4.82
cinnamic acid	17.9	3.3	8.7	4.15	6.32
Citric Acid	18.5	5.1	20.2	12.80	13.30
ferulic acid	18.8	5	14.6	7.31	7.93
Fumaric acid	17	6.9	15.3	8.39	9.72
Gallic Acid	22.6	6.4	25.5	18.05	18.42
glutaric acid	17.3	3.9	13.6	7.19	9.34
hippuric acid	19.2	6.5	10.4	3.01	3.49
Maleic acid	17	4.9	15.3	8.53	10.57
Malonic Acid	17.8	5.6	16.3	9.10	10.19
Nicotinamide	16.4	11.1	12.4	7.71	5.67
Nicotinic acid	17	9.5	12.6	6.70	6.21
oxalic acid	18	10.1	18.4	11.61	10.88
p-amino benzoic acid	19.5	4.1	13.1	6.05	6.16
Resorcinol	18	5.4	20.7	13.35	14.04
Saccharin	19.4	7	6.7	1.37	1.65
succinic acid	17.5	6.5	14.8	7.73	8.94
Tartaric acid	17.1	9.6	25	17.96	17.73
Urea	17.1	11	19.4	13.03	11.96
Vanillic acid	20.2	6.2	16.2	8.61	8.61
Xanthine	19.9	15.5	14.2	11.17	10.23
Xylitol	14	6	27.6	20.97	23.41

Table 4. Summary Table of Dispersive, Polar and Hydrogen Bonding Forces and Solubility Parameters for tideglusib and coformer candidates using Van Krevelen Methodology

Table 5: Aromatic coformer candidate physicochemical properties

Coformer	MW (g/mol)	m.p. (°C)	Molecular Structure	H-Bond Donors	H-bond Acceptors
Vanillic Acid	168.14	211.5	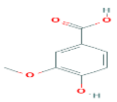	2	4
Resorcinol	110.112	111	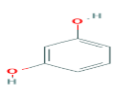	2	2

Table 5: Aromatic coformer candidate physicochemical properties

Coformer	MW (g/mol)	m.p. (˚C)	Molecular Structure	H-Bond Donors	H-bond Acceptors
Benzoic Acid	122.123	122	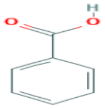	1	2
Cinnamic Acid	148.161	133	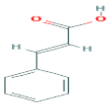	1	2
Hippuric Acid	179.175	191.5	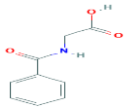	2	3
1-Hydroxy-2-Naphthoic Acid	188.182	195	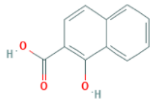	2	3
Catechol	110.112	105	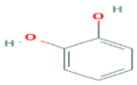	2	2
Ferulic Acid	194.186	168-171	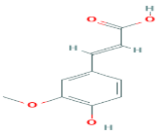	2	4
p-amino-benzoic Acid	137.138	188.5	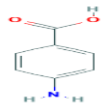	2	3
Anthranilic Acid	137.138	146-148	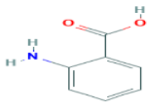	2	3
Gallic Acid	170.12	260	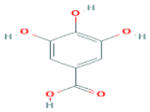	4	5
Nicotinamide	122.12	128	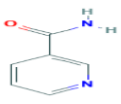	1	2
Nicotinic Acid	123.11	237	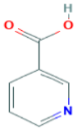	1	3

Table 5: Aromatic coformer candidate physicochemical properties

Coformer	MW (g/mol)	m.p. (˚C)	Molecular Structure	H-Bond Donors	H-bond Acceptors
Saccharin	183.18	229-230	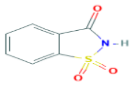	1	3
Xanthine	152.11	>300	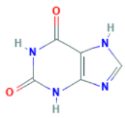	3	6
Caffeine	194.19	236.5	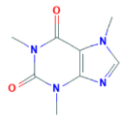	0	6

Table 6: Non-aromatic coformer candidate physicochemical properties

Coformer	MW (g/mol)	m.p. (˚C)	Molecular Structure	H-Bond Donors	H-bond Acceptors
Adipic Acid	**146.142**	**152**	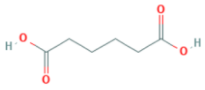	**2**	**4**
Glutaric Acid	**132.115**	**98**	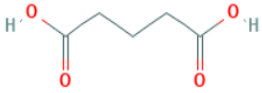	**2**	**4**
Succinic Acid	**118.088**	**188**	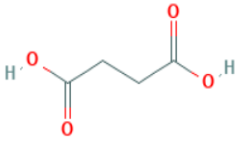	**2**	**4**
Urea	**60.056**	**133-135**	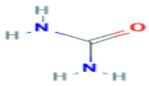	**2**	**1**
Citric Acid	**192.124**	**153**	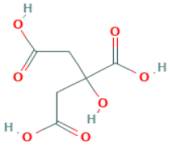	**4**	**7**

Malonic Acid	**104.061**	**135-137**	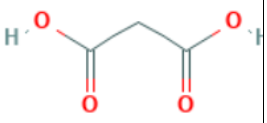	**2**	**4**
Oxalic Acid	**90.03**	**190**	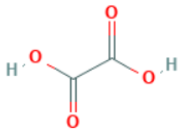	**2**	**4**
Xylitol	**152.15**	**92-96**	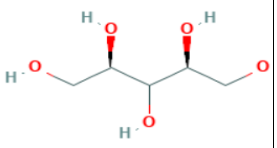	**5**	**5**
D,L-tartaric acid	**150.09**	**171-174**	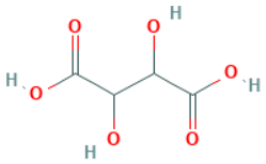	**4**	**6**
Fumaric Acid	**116.07**	**287**	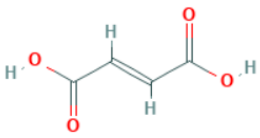	**2**	**4**
Maleic Acid	**116.07**	**135**	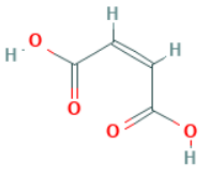	**2**	**4**

Materials and Methods

Micronized tideglusib (purity: ≥99.0%) was provided by AMO Pharma Ltd. All coformer candidates were sourced from Sigma-Aldrich as follows: 1-hydroxy-2-naphthoic acid (purity ≥97.0%, actual: 99.7%), resorcinol (purity ≥99.0%, actual: 99.8%), trans-cinnamic acid (purity ≥99%, actual: 99.7%), vanillic acid (purity ≥97.0%, actual: 99.3%), adipic acid (purity ≥99.5%, actual: 99.7%), benzoic acid (purity ≥99.5%, actual: 100.2%), glutaric acid (purity: 99%, actual: 99.6%), hippuric acid (purity: 98%, actual: 99.6%), 1,2-dihydroxybenzene (purity ≥99%, actual: 99.7%), trans-ferulic acid (purity: 99%, actual: 99.7%), 4-aminobenzoic acid (purity ≥99%, actual: 100%), anthranilic acid (purity: ≥98%, actual: 99.9%), succinic acid (purity ≥99.0%, actual: 99.8%), gallic acid (purity: 97.5-102.5%, actual: 100.0%), urea (purity: 98.0-102.0%, actual: 101.0%), nicotinamide (purity: ≥99.5%, actual: 99.9%), citric acid (purity: ≥99.5%, actual: 99.8%), malonic acid (purity: 99%, actual: 99.9%), oxalic acid (purity: ≥99%, actual 99.8%), saccharin (purity: ≥98%, actual: 100.0%), nicotinic acid (purity: ≥99.5%, actual: 99.5%), xanthine (purity: ≥99%, actual 100%), caffeine (purity: ≥99.0%, actual: 100.0%), xylitol (purity: ≥99%, actual 100%), D,L-tartaric acid (purity: 99%, actual 99.4%), fumaric acid (purity: ≥99.0%, actual: 100.0%), maleic acid (purity: ≥99%, actual: 100%).

Purity levels were quoted from certificates of analysis and accepted as reported.

Sample Preparation

Binary mixtures of drug and coformer prepared in 1:1 stoichiometric ratio (target: 0.01 moles). using mechanical co-grinding. The co-grinding approach attempted to (1) maximize uniformity in solid state powder mixing and (2) improve the probability of detection of an interaction within each binary system. Samples were first physically mixed for no less than 2 minutes in a Pyrex® borosilicate glass mortar and pestle. The mixture was then co-ground with the pestle in two identical repeated steps. Each step involved grinding for no less than 60 seconds. Between co-grinding steps 1 and 2, the co-ground material was collected from the walls of the mortar, using a spatula, reintroduced to the bowl, and physically mixed again for 60 seconds.

Differential Scanning Calorimetry (DSC)

DSC was performed using a TA Instruments Discovery DSC 2500 series (with Trios Software). Software enabled characterization of endotherms. While a new endotherm below the melting point of both materials is indicative of a eutectic, one developing between the two material melting points may indicate co-crystal formation, this is not always the case. This is highlighted for 50 co-crystal systems in the review by Schultheiss and Newman where 51% cocrystals had melting points between those of the API and coformer, but 39% were lower than either the API or coformer (Schultheiss and Newman 2009). For reference, DSC scans were performed for tideglusib, each coformer to determine enthalpy of fusion ($\Delta_{fus}H$) and to study the potential for independent behaviors such as polymorphism , sublimation ($\Delta_{sub}H$) and/or decomposition thus affording meaningful inference of the resulting data. Samples were prepared using T_{zero} Aluminum (Al) pan/lid configuration. Samples were equilibrated at 25°C, and then heated (5°C/min) to maximum temperatures, followed by equilibration. First heat cycle data was used for the evaluation of binary interaction, while cooldown and subsequent heat cycle data was generated to further characterize the system when necessary. Trios software recorded melting onsets, melting points and both endothermic and exothermic transitions. Theoretical expected enthalpic contributions (J/g) to a melting endotherm were calculated by weight-adjusted normalizing the enthalpies of neat material to the theoretical expected composition in the sample at the respective melting temperature. Theoretical enthalpic values were then compared to actual calculated enthalpy to determine the extent (%) of interaction. Interactions of 0-15% fall within assumed content uniformity variance i.e., a slightly reduced endotherm peak area (enthalpy) of 10% may be due to lower than target sample content. In such cases, (1) tideglusib endotherm peak characteristics were examined for evidence of melting point depression i.e., where colligative properties of solubilized coformer infer an interaction and (2) complementing examination of the coformer melting behavior for enthalpic loss or melting point depression.

RESULTS & DISCUSSION

Qualitative and Quantitative Analyses of DSC Thermograms

DSC thermograms were generated for tideglusib and all 27 binary systems. These quantitative data are summarized in **Table 7** and **Table 8** for tideglusib and coformer observations. Actual DSC thermograms are available as supplemental data.

Experiment	Tideglusib Content Factor	Theoretical contribution to tideglusib melting	Actual contribution to tideglusib melting	% tideglusib endotherm loss	Eutectic Binary Outcome	Interaction Binary Outcome

		enthalpy (J/g) at tideglusib melting point	enthalpy (J/g) at tideglusib melting point			
Tideglusib	1.000	110	110	-	-	-
benzoic acid	0.734	81	17	78	1	1
cinnamic acid	0.691	76	2	98	1	1
1-hydroxy-2-naphthoic acid	0.639	70	0	100	1	1
anthranilic acid	0.710	78	0	100	1	1
p-amino benzoic acid	0.709	78	0	100	1	1
Vanillic acid	0.665	73	0	100	1	1
ferulic acid	0.631	70	0	100	1	1
1,2-dihydroxybenzene	0.747	82	11	89	1	1
hippuric acid	0.654	72	0	100	1	1
nicotinamide	0.731	81	0	100	1	1
resorcinol	0.732	81	6	94	1	1
adipic acid	0.686	76	0	100	1	1
gallic acid	0.661	73	69	6 [1]	0	1 [1]
glutaric acid	0.720	79	0	100	1	1
saccharin	0.645	71	0	100	1	1
succinic acid	0.737	81	0	100	1	1
malonic acid	0.761	84	0	100	1	1
citric acid	0.634	70	65	7	0	0
Urea	0.845	93	89	5	0	0
oxalic acid	0.787	87	0	100	1	1
Nicotinic Acid	0.730	80	77	4 [2]	0	1 [2]
Xanthine	0.685	76	65	14	0	0
Caffeine	0.632	70	0	100	1	1
Xylitol	0.688	76	72	5	0	0
D,L-tartaric acid	0.687	76	71	6	0	0
Fumaric Acid	0.741	82	78	4 [3]	0	1 [3]
Maleic Acid	0.739	82	0	100	1	1

1: Corresponding free gallic acid melting endotherm is lost to new lower melting endotherm. Interaction concluded through coformer melt behavior.

2: Tideglusib melt endotherm displays melting point depression. Corresponding free nicotinic acid melting endotherm lost to new lower melting endotherm. Interaction concluded.

3: Corresponding free fumaric acid melting endotherm lost to new lower melting endotherm. Interaction concluded through coformer melt behavior.

Table 7– Quantitative Assessment Of Eutectic and Interaction Outcomes - Tideglusib

Experiment	Coformer enthalpy (J/g)	Coformer Factor	Theoretical contribution to coformer melting enthalpy (J/g) at coformer melting point	Actual contribution to coformer melting enthalpy (J/g) at coformer melting point	% coformer endotherm loss	Interaction Binary Outcome
benzoic acid	150	0.266	40	35	13	1 [1,2]
cinnamic acid	137	0.309	42	16	63	1
1-hydroxy-2-naphthoic acid	210	0.361	76	0	100	1
anthranilic acid	158	0.290	46	1	98	1
p-amino benzoic acid	188	0.291	55	0	100	1
Vanillic acid	161	0.335	54	0	100	1
ferulic acid	170	0.369	63	0	100	1
1,2-dihydroxybenzene	240	0.253	61	27	55	1
hippuric acid	191	0.346	66	0	100	1
nicotinamide	202	0.269	54	0	100	1
resorcinol	187	0.268	50	9	83	1
adipic acid	237	0.314	74	0	100	1
gallic acid	182	0.339	62	0	100	1
glutaric acid	186	0.280	52	60	(14)	1 [1,3]
saccharin	166	0.355	59	0	100	1
succinic acid	288	0.263	76	0	100	1
malonic acid	242	0.239	58	0	100	1
citric acid	242	0.366	89	>72	<19	0 [4]
Urea	250	0.155	39	56	0	0
oxalic acid	989 [5]	0.213	211	0	100	1
Nicotinic Acid	230 [6]	0.270	62	0 [6]	100	1
Xanthine	N.P.[7]	0.315	N.P.	119	0	0
Caffeine	137	0.368	50	0	100	1
Xylitol	237	0.312	74	81	0	0
D,L-tartaric acid	334 [8]	0.313	105	N.P. [8]	N.P.	0
Fumaric Acid	1065	0.259	279	0	100	1
Maleic Acid	1139 [5]	0.261	297	0	100	1

1: Refer to tideglusib result.

2: Benzoic acid melting endotherm significantly broadened (onset 115C vs 122C), suggesting reduced crystallinity and interaction.

3: Glutaric acid melting endotherm displaying melting point depression (onset: 95C vs 97C, melting: 96C vs 98C).

4: Peak integration under-reported error. Actual enthalpy Approximates to theoretical. Total actual enthalpy vs theoretical (157.2 J/g vs 158.4 J/g). Therefore, no interaction.

5: Calculated enthalpy values for oxalic acid and maleic acid agree with literature for behaviors consistent with melting and/or sublimation with decomposition. 6. Nicotinic acid enthalpy of fusion ($\Delta_{fus}H$) of 26.7 – 30.0kJ/mol (from literature). Sublimation reported. Interaction due to new endotherm at temperature below free fumaric acid. 7: Determination of enthalpy of melting for free xanthine was not possible due to observed decomposition. Endotherm detected in binary co-grind, however. 8: Melts with decomposition. Value therefore approximate. Not determinable in the co-grind.
Table 8- Quantitative Assessment Of Eutectic and Interaction Outcomes - Coformers

General Observations Of Interactions & Eutectic Formation

Refer to **Table 7** and **Table 8**. A review of all 27 experiments resulted in the following conclusions. 81% (22/27) of binary experiments demonstrated an interaction, while eutectics were detected for 70% (19/27) of the experiments.

For the 7 'control' co-formers where δ(δTotal) > 10MPa$^{1/2}$, 5/7 (71%) behaved as expected and did not interact. However, two controls, oxalic acid and malonic acid showed evidence of an interaction. Both experiments resulted in a lower melting endotherm, indicative of a eutectic. It is noted, however, that results may be confounded by potential decomposition with concommittant formation of carbon dioxide and either formic acid or acetic acid, respectively. For oxalic acid, literature reports DTA/TGA formation of an anhydrous form at ~190°C with subsequent decomposition (Fischer, Scholz et al. 2015). The decomposition products are formic acid and carbon dioxide, and additional literature references report sublimation and onset of degradation at lower temperatures (>149°C). Literature also reports (Bradley and Cleasby 1953) sublimation of oxalic acid, $\Delta_{sub}H°$ = 97.906 kJ/mol (1087.48 J/g) and this was assessed by integrating a repeat DSC sample of oxalic acid from 100°C (after hydrate loss) through 210°C. The value was in good agreement (988.66 J/g). As a result, analysis of the co-grind sample must therefore consider deviations in enthalpy due to potential changes in mass and heat capacity due to instability, co-grind processing or interactions. This is consistent with the approach to experimental analysis for the tideglusib/malonic acid binary system because malonic acid and oxalic acid are closely related dicarboxylic acid molecules, differing only in a -CH_2 group between the carboxylic acids. The solubility parameters for oxalic acid are reiterated as δD: 17.8, δP: 13.8, δH: 26.2, with a δTotal: 34.55 MPa$^{1/2}$. For reference, tideglusib possesses a δTotal of 21.62 MPa$^{1/2}$. This constitutes a δ(δTotal): 12.93. By comparison, formic acid reports solubility parameters of: δD: 14.2, δP: 8.6, δH: 13.3, with a δTotal: 21.27 MPa$^{1/2}$. This is practically identical to the δTotal for tideglusib (δ(δTotal): 0.35 MPa$^{1/2}$). Therefore, a compositional change with an increase in the concentration of formic acid, if occurring, could significantly confound the experimental results due to a substantial increase in miscibility. Similarly, malonic acid decomposes to acetic acid and carbon dioxide at ~140°C (Bank 2018). Co-grind sample analysis was likely confounded due to changes in mass and heat capacity. Specifically, malonic acid reports solubility parameters as follows: δD: 17.5, δP: 11.9, δH: 24.2, with a δTotal: 32.15 MPa$^{1/2}$. This constitutes a δ(δTotal): 10.53. By comparison, acetic acid reports solubility parameters of: δD: 15.2, δP: 6.6, δH: 13.6, with a δTotal: 21.44 MPa$^{1/2}$. This is again practically identical to the δTotal for tideglusib (δ(δTotal): 0.18 MPa$^{1/2}$). Like oxalic acid, the presence of decomposition products could result in miscibility of tideglusib at the melting point range of malonic acid. It is therefore possible that immiscibility occurs for all 7 controls. However, a supplementary analysis by TGA would be required before invalidating the empirically observed miscibility.

For the remaining 20 coformer, where interaction was expected or probable, 100% (20/20) interacted. For eutectic formation,

17/20 were successful. The three coformers that interacted without eutectic formation were: nicotinic acid, fumaric acid, and gallic acid. Surprisingly, the HSP distance between tideglusib and nicotinic acid is small (δ(δTotal): 3.06 $MPa^{1/2}$). As such, miscibility and eutectic formation was expected but not observed. Fumaric acid , trans-isomer of the unsaturated dicarboxylic acid (butenedioic acid) did not form a eutectic while the cis-isomer, maleic acid, (identical HSP distance δ(δTotal): 9.64 $MPa^{1/2}$) did. The reasons for one isomer forming a eutectic while the other does not are not yet understood. While it is a stronger acid, it is less stable than fumaric acid and melts at lower temperature, presumably due to greater intramolecular rather than intermolecular hydrogen bonding. Maleic acid may also undergo chemical change upon melting to form the anhydride (with water loss), thus confounding the observations. The nature of the interaction between fumaric acid and tidegluisb is an early partitioning of the coformer into molten tideglusib i.e. melting point depression. However, no melting point depression was observed for tideglusib which melts ~150°C lower than free fumaric acid. A possible explanation is that the δ(δTotal): 9.64 $MPa^{1/2}$ is borderline in terms of suspected miscibility and that fumaric acid, the trans-isomer, with greater intermolecular hydrogen bonding with neighboring fumaric acid molecules, is less available to interact with tideglusib until closer to the melting point. Similarly, gallic acid is a high melting point acid (260°C) and may not give up strong intermolecular hydrogen bonding at temperatures below melting.

These observations, particularly for malonic acid, oxalic acid and the cis and trans-isomers, demonstrate some limitations of reliance on a solubility parameter alone and without further context. While the model cannot fully predict all outcomes, the success rate is nevertheless excellent.

Data Treatment

Per **Table 7** and **Table 8**, the authors estimated the degree of interaction for tideglusib and each coformer. To reiterate, for minor deviations from theoretical by <15%, content uniformity was suspected. To remove the noise of content uniformity, experimental outcomes were assigned a binary score (1: interaction, 0: no interaction). This treatment was followed for two conditions, (1) interaction via melting point depression and/or early melting/partitioning of higher melting coformer or eutectic formation, and (2) a more selective investigation of eutectic formation only.

In summary, for the 27 experiments, 22 coformers showed evidence of an interaction with tideglusib. Only citric acid, urea, xanthine, xylitol and D,L-tartaric acid were non-interacting. Of the 22 interacting coformers, 19 showed evidence of eutectic formation. Only gallic acid, nicotinic acid, fumaric acid did not display any sign of eutectic formation.

Interaction Binary Outcome – Graphical Analysis

Five separate binary fitted line plots were prepared using Minitab (2019) software (logit function, $\alpha = 0.05$ two-sided). Independent variables were derived from the Y-MB values i.e., δ(δTotal), Δδ-Y-MB, and Ra(v)-Y-MB, as well from Van Krevelen values, namely, Δδ, and Ra(v). The dependent variable was interaction (0,1) (Figure 5**)**. Due to the limited data sets (n=1 per experiment), no assessment of statistical significance is proposed for this analysis. Yet, it is empirically demonstrated that the probability of an interaction follows an expected relationship and this relationship undergoes a marked shift as distances cross threshold values. This is intuitive and agrees with the general literature findings for the correlation of HSP and miscibility (Mohammad, Alhalaweh et al. 2011) (Nagy, Pál et al. 2019).

Interaction as a function of δ(δTotal)

In the case of δ(δTotal) fitted plot, (adjusted R^2: 75%), values of δ(δTotal) <8 $MPa^{1/2}$ appear to trend well with probability of interaction. As this threshold limit is exceeded, a finding of non-interaction is increasingly possible.

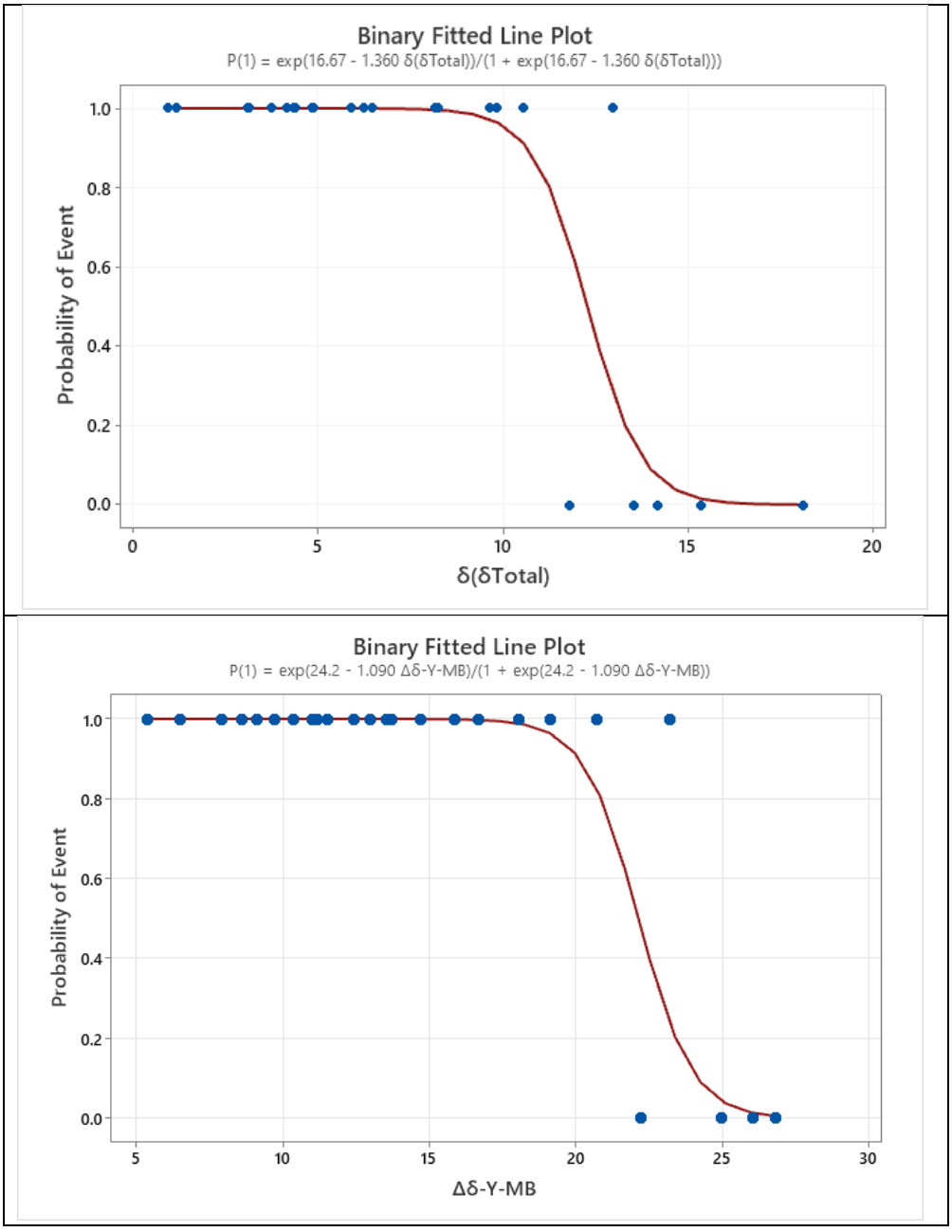
Binary Fitted Line Plot
P(1) = exp(16.67 - 1.360 δ(δTotal))/(1 + exp(16.67 - 1.360 δ(δTotal)))
Probability of Event
1.0
0.8
0.6
0.4
0.2
0.0
0
5
10
15
20
δ(δTotal)
Binary Fitted Line Plot
P(1) = exp(24.2 - 1.090 Δδ-Y-MB)/(1 + exp(24.2 - 1.090 Δδ-Y-MB))
Probability of Event
1.0
0.8
0.6
0.4
0.2
0.0
5
10
15
20
25
30
Δδ-Y-MB

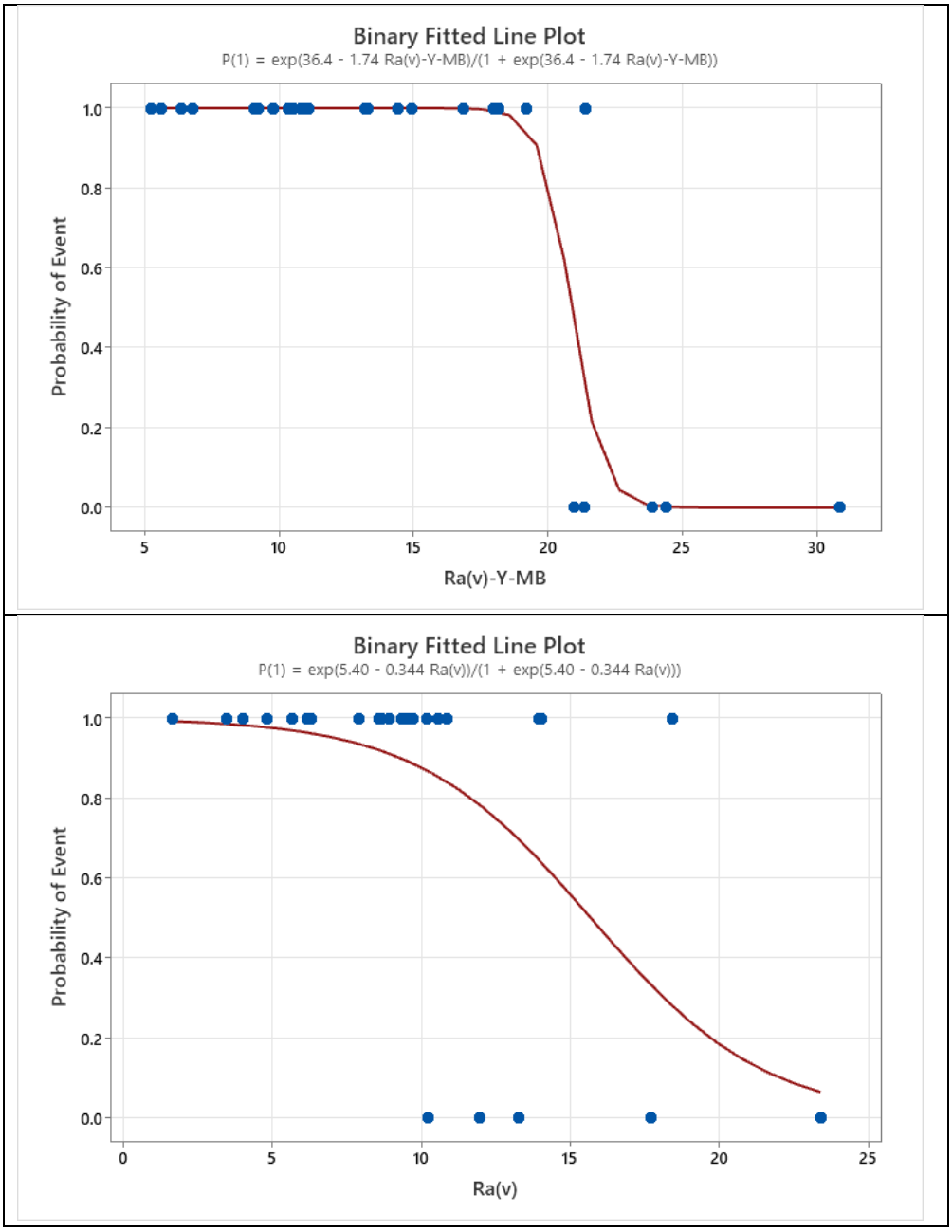
Binary Fitted Line Plot
P(1) = exp(36.4 - 1.74 Ra(v)-Y-MB)/(1 + exp(36.4 - 1.74 Ra(v)-Y-MB))
Probability of Event
1.0
0.8
0.6
0.4
0.2
0.0
5
10
15
20
25
30
Ra(v)-Y-MB
Binary Fitted Line Plot
P(1) = exp(5.40 - 0.344 Ra(v))/(1 + exp(5.40 - 0.344 Ra(v)))
Probability of Event
1.0
0.8
0.6
0.4
0.2
0.0
0
5
10
15
20
25
Ra(v)

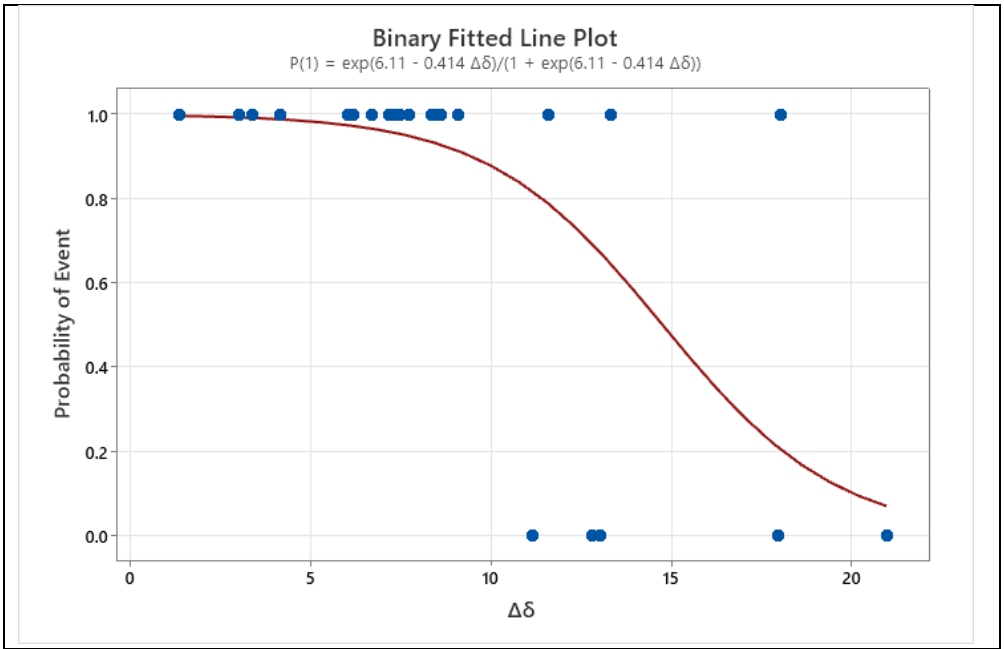

Figure 5 Binary Fitted Plot: Probability of Interaction/Miscibility vs δ(δTotal), Δδ-Y-MB, Ra(v)-Y-MB, Ra(v), Δδ

Interaction as a function of Δδ-Y-MB

In the case of Δδ-Y-MB, (adjusted R^2: 72%), values <17 $MPa^{1/2}$ appear to trend well with probability of interaction. As this threshold limit is exceeded, a finding of non-interaction is increasingly possible.

Interaction as a function of Ra(v)-Y-MB

In the case of the Ra(v)-Y-MB an adjusted R^2 value (78%) was determined. The probability of an interaction is increasingly likely when Ra(v)-Y-MB < 17$MPa^{1/2}$.

Similar exercises were evaluated for δD, δP, δH, δHA, and δHD (not presented). Relationships were evident for all but δD. However, the data and curve fitting does not adequately explain the variance (adj R^2 values: 23-39%).

Interaction as a function of Ra(v) – Van Krevelen

For the Radius of Interaction (Ra(v)) (adjusted R^2: 28%), positive interactions were empirically reported at Ra(v) values <10 $MPa^{1/2}$. However, the change between interaction and non-interaction is not as clear as that observed for Y-MB derived parameters. The non-interaction at Ra(v) = 10.23, 11.96,13.30 $MPa^{1/2}$, for xanthine, urea, and citric acid, coupled with the interacting values of 13.33, 13.35, and 18.05 $MPa^{1/2}$ for 1,2-dihydroxybenzene, resorcinol and gallic acid, and the resulting low adjusted R^2 value, suggest a relationship less defined by this parameter. In fact, a threshold may be exceeded at values much less than 10$MPa^{1/2}$.

Interaction as a function of Δδ – Van Krevelen

For Δδ, the binary fitted plot presents an adjusted R^2: 36%. Positive interactions were reported at Δδ values < 9 $MPa^{1/2}$ but with increasing probability of non-interactions beginning at lower values. In the region of 11 – 18 $MPa^{1/2}$, the model does not adequately predict interaction vs. non-interaction.

Eutectic Binary Outcome – Statistical & Qualitative Analysis

For the dependent variable of eutectic formation, ten continuous variables were assessed. Eight were derived from Y-MB values: δ(δTotal), Δδ-Y-MB, Ra(v)-Y-MB, δ(δD), δ(δP), δ(δH), δ(δHD), δ(δHA). Those derived from Van Krevelen methodology values, were, Δδ, and Ra(v).

A logistical regression model was employed using SAS studio – University edition 2021, logit function, alpha = 0.05 two-sided. Maximum likelihood estimates method was

used to determine the parameters for the models. The function can be described as per **Equation 6**.

From this equation, the incremental increase in odds for a single unit increase in X can be determined and the odds ratio i.e., occurrence over non-occurrence at any given value of X can be calculated. Logistical regression data are presented in **Table 9, Table 10, Figure 6**.

$\log(p/(1-p)) = \text{logit}(p) = \beta0 + \beta1*(X)$ **Equation 6**
Where: p = probability of occurrence, 1-p = probability of non-occurrence and (p/(1-p)) = odds ratio β0 = intercept of the logit function, corresponding to log(odds) of a coformer with distance '0' having no eutectic formation β1 = log odds point estimate X = δ(δTotal), Δδ-Y-MB, Ra(v)-Y-MB, δ(δD), δ(δP), δ(δH), δ(δHD), δ(δHA), Δδ, or Ra(v)

Effect	**Point Estimate**	**95% Wald Confidence Limits**	
δ(δD) [1]	1.208	0.578	2.522
δ(δP) [1]	1.220	0.990	1.504
δ(δTotal)	1.476	1.102	1.977
Δδ-Y-MB	1.274	1.055	1.540
Ra(v)-Y-MB	1.271	1.047	1.543
δ(δH)	1.234	1.029	1.479
δ(δHD)	1.298	1.038	1.623
δ(δHA)	1.364	1.048	1.776
Ra(v)	1.424	1.058	1.917
Δδ	1.502	1.092	2.068

Table 9: Odds Ratio Estimates

1: Not statically significant at alpha = 0.05

Table 9 summarily presents the point estimates for the odds ratio for each model and the corresponding confidence intervals about these point estimates. Table 10 summarily presents the logit function data, as derived from the analyses of maximum likelihood estimates including β_0, β_1, and statistical significance using the Wald X^2 function.

Parameter	DF	Estimate	Standard Error	Wald Chi-Square	Pr > ChiSq
Intercept	1	-1.2123	0.7390	2.6913	0.1009 [1]
δ(δD)	1	0.1886	0.3758	0.2517	0.6159 [1]
Intercept	1	-2.2924	0.8772	6.8296	0.0090
δ(δP)	1	0.1988	0.1067	3.4688	0.0625 [1]
Intercept	1	-4.2267	1.4664	8.3078	0.0039
δ(δTotal)	1	0.3894	0.1490	6.8284	0.0090
Intercept	1	-4.9480	1.8012	7.5464	0.0060
Δδ-Y-MB	1	0.2425	0.0966	6.3070	0.0120
Intercept	1	-4.7167	1.7486	7.2760	0.0070
Ra(v)-Y-MB	1	0.2402	0.0989	5.8982	0.0152
Intercept	1	-3.8445	1.4688	6.8506	0.0089
δ(δH)	1	0.2101	0.0925	5.1538	0.0232
Intercept	1	-4.8840	1.9418	6.3263	0.0119
δ(δHD)	1	0.2607	0.1142	5.2132	0.0224
Intercept	1	-3.1430	1.1162	7.9289	0.0049
δ(δHA)	1	0.3107	0.1345	5.3365	0.0209
Intercept	1	-4.5654	1.6936	7.2672	0.0070
Ra(v)	1	0.3536	0.1517	5.4348	0.0197
Intercept	1	-4.9735	1.7644	7.9451	0.0048
Δδ	1	0.4071	0.1629	6.2435	0.0125

Table 10: Analysis of Maximum Likelihood Estimates

1: Not statistically significant at $\alpha = 0.05$

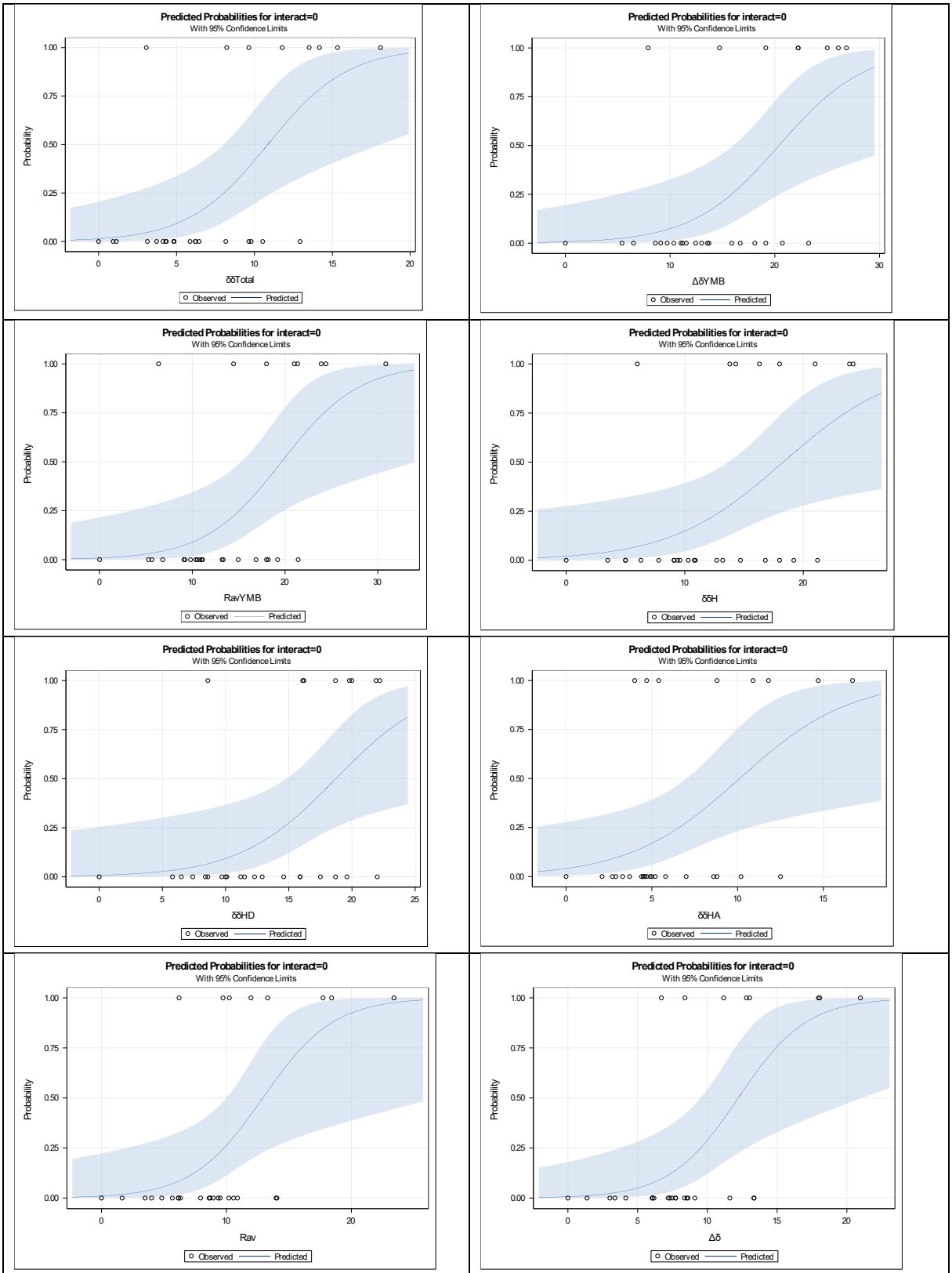

Figure 6: Predicted Probabilities of Eutectic Formation as f(distance from tideglusib). 0 = Eutectic; 1 = No Eutectic.

From **Figure 6**, as distances decreases the probability of eutectic formation ('interaction') **NOT** occurring, approaches zero '0'. Conversely, as distances increase (left to right), the probability of eutectic formation **NOT** occurring, becomes increasingly probable. This is correct since

eutectics occur through effective miscibility. Multi-regression modelling was not performed due to concerns with multicollinearity distance and the underlying δD, δP, δH force values, and δH and δHA and δHD.

Eutectic Formation as a function of Y-MB derived HSP parameters of δ(δTotal), Δδ-Y-MB, Ra(v)-Y-MB, δ(δD), δ(δP), δ(δH), δ(δHD), δ(δHA)

Statistically significant relationships were determined for δ(δTotal), Δδ-Y-MB, and Ra(v) – Y-MB, δ(δH), δ(δHD), and δ(δHA) (p-value: β_0: 0.0039 – 0.0119; p-value: β_1: 0.0090 – 0.0232, α = 0.05). However, the relationship between eutectic formation and either δ(δD) or δ(δP) was not significant. Hydrogen bonding force may therefore be key to tideglusib eutectic formation. This is also confirmed for hydrogen bond donor and acceptor character. Data presented in **Table 10** was used to create probability predictions for each function. **Table 11** presents the predicted probabilities for each continuous variable, for arbitrarily selected distances of 2, 5, 10, 15, 20 and 30 $MPa^{1/2}$. The relative changes in probabilities of eutectic formation/non-formation present useful insight in identifying appropriate thresholds that may be considered when screening coformers for eutectic formation. These thresholds will differ based on the selected solubility parameter and methodology. For δ(δTotal) significant changes occur between values of 5 $MPa^{1/2}$ (1-p = 0.907) and 10 $MPa^{1/2}$, (1-p = 0.582) with extremely low probability of eutectic formation as δ(δTotal) pass 15 $MPa^{1/2}$ (1-p = 0.166).

For Δδ-Y-MB, and Ra(v) – Y-MB, corresponding significant changes do not occur until distance values approach and then exceed a threshold of 15 $MPa^{1/2}$ and probabilities of ~0.5 are predicted at ~20 $MPa^{1/2}$. The values for δ(δH) and δ(δHD) follow a similar function to these values while the differences in hydrogen bond accepting forces (δ(δHA)) are more sensitive to changes and follow a similar course dependence to δ(δTotal).

Empirically, out of 18 coformers with δ(δTotal) <10 $MPa^{1/2}$, there were 16 eutectics formed (success rate: 89%). This is slightly higher than the predicted values. However, for the remaining design space, where 10 $MPa^{1/2}$ < δ(δTotal) < 24 $MPa^{1/2}$, there were 3 eutectics formed and 6 that did not form (success rate: 33%). This is consistent with the model values of 1-p = 0.166 – 0.582.

Scores for Δδ-Y-MB, Ra(v)-Y-MB are consistent with 6/7 (86%) and 7/8 (88%) successful eutectics formed, respectively, when values are < 10 $MPa^{1/2}$. In both cases, if the limits are expanded to NMT 15 $MPa^{1/2}$, the success rates remain consistent with 13/15 (87%) and 14/16 (88%) for Δδ-Y-MB and Ra(v)-Y-MB, respectively. In fact, failures rates only increase when values begin to exceed a threshold approaching 20 $MPa^{1/2}$.

Due to the significance of the relationship between hydrogen bonding and interactions and eutectic formation, this analysis was also performed for δ(δH), δ(δHA) and δ(δHD). Out of 11 coformers with δ(δH) <10 $MPa^{1/2}$, there were 10 eutectics formed (success rate: 91%). For the remaining design space, where 10$MPa^{1/2}$ < δ(δH)< 24 $MPa^{1/2}$, there were 9 eutectics formed and 7 that did not form (success rate: 56%). There were 20 coformers with δ(δHA) <10 $MPa^{1/2}$ and the success rate were 17/20 (85%); where 10$MPa^{1/2}$ < δ(δHA)< 20 $MPa^{1/2}$, the success rate was 2/7 (29%). Finally, there were 9 coformers with δ(δHD) <10 $MPa^{1/2}$ and the success rate was 8/9 (85%). For the 18 coformers where 10$MPa^{1/2}$ < δ(δHD)< 24 $MPa^{1/2}$, the success rate was 11/18 (61%).

Interestingly, δ(δD) (dispersion force differences) only ranged from 0.1 – 3.5 $MPa^{1/2}$ across the entire 27 coformer design space. The qualitative assessment of eutectic success rate across this narrow range yielded the same conclusion as the statistical assessment where eutectic success and failures rates did not correlate with distance. Half (4 of the 8) eutectic failures occurred in the 10 closest coformers (0.1 – 0.8 $MPa^{1/2}$). Similarly, for δ(δP) (polar force differences), while the range of values was 0.5 – 22.7 $MPa^{1/2}$, more than half (5 of the 8) eutectic failures occurred when 0.5$MPa^{1/2}$ < δ(δP)< 6.8 $MPa^{1/2}$.

	δ(δTotal)	Δδ-Y-MB	Ra(v) – Y-MB	δ(δH)	δ(δHD)	δ(δHA)	Ra(v)	Δδ
β0	-4.2267	-4.948	-4.7167	-3.8445	-4.884	-3.143	-4.5654	-4.9735
β1	0.3894	0.2425	0.2402	0.2101	0.2607	0.3107	0.3536	0.4071
logit(p), X=2	-3.448	-4.463	-4.236	-3.424	-4.363	-2.522	-3.858	-4.159
(p/1-p), X=2	0.032	0.012	0.014	0.033	0.013	0.080	0.021	0.016
p, X=2 (no eutectic)	0.031	0.011	0.014	0.032	0.013	0.074	0.021	0.015
1-p, X=2 (eutectic)	0.969	0.989	0.986	0.968	0.987	0.926	0.979	0.985
logit(p), X=5	-2.280	-3.736	-3.516	-2.794	-3.581	-1.590	-2.797	-2.938
(p/1-p), X=5	0.102	0.024	0.030	0.061	0.028	0.204	0.061	0.053
p, X=5 (no eutectic)	0.093	0.023	0.029	0.058	0.027	0.169	0.057	0.050
1-p, X=5 (eutectic)	0.907	0.977	0.971	0.942	0.973	0.831	0.943	0.950
logit(p), X=10	-0.333	-2.523	-2.315	-1.744	-2.277	-0.036	-1.029	-0.903
(p/1-p), X=10	0.717	0.080	0.099	0.175	0.103	0.965	0.357	0.406
p, X=10 (no eutectic)	0.418	0.074	0.090	0.149	0.093	0.491	0.263	0.289
1-p, X=10 (eutectic)	0.582	0.926	0.910	0.851	0.907	0.509	0.737	0.711
logit(p), X=15	1.614	-1.311	-1.114	-0.693	-0.974	1.518	0.739	1.133
(p/1-p), X=15	5.024	0.270	0.328	0.500	0.378	4.561	2.093	3.105
p, X=15 (no eutectic)	0.834	0.212	0.247	0.333	0.274	0.820	0.677	0.756
1-p, X=15 (eutectic)	0.166	0.788	0.753	0.667	0.726	0.180	0.323	0.244
logit(p), X=20	3.561	-0.098	0.087	0.358	0.330	3.071	2.507	3.169
(p/1-p), X=20	35.209	0.907	1.091	1.430	1.391	21.563	12.263	23.772
p, X=20 (no eutectic)	0.972	0.476	0.522	0.588	0.582	0.956	0.925	0.960
1-p, X=20 (eutectic)	0.028	0.524	0.478	0.412	0.418	0.044	0.075	0.040
logit(p), X=30	7.455	2.327	2.489	2.459	2.937	6.178	6.043	7.240
(p/1-p), X=30	1729.003	10.247	12.053	11.687	18.859	482.027	420.986	1393.397
p, X=30 (no eutectic)	0.999	0.911	0.923	0.921	0.950	0.998	0.998	0.999
1-p, X=30 (eutectic)	0.001	0.089	0.077	0.079	0.050	0.002	0.002	0.001

Table 11: Estimating Probabilities of Eutectic Interaction as f(distance measurement)

Eutectic Formation as a function of Van Krevelen derived HSP parameters of Ra(v), Δδ

Statistically significant relationships were determined between Ra(v), and Δδ and the formation of a eutectic (p-value: β_0: 0.0070 – 0.0048; p-value: β_1: 0.0125 – 0.0197, $\alpha = 0.05$). The estimates for β_0 and β_1 and the resulting odds ratio and predicted probabilities are also presented in **Table 11**.

As the values of Ra(v), and Δδ increase from 2, 5, 10, 15, 20 through 30 $MPa^{1/2}$, the predicted probability of eutectic formation drops from 0.979, 0.943, 0.737, 0.323, 0.075, to 0.002 for Ra(v) and from 0.985, 0.950, 0.711, 0.244, 0.040, to 0.001 for Δδ, respectively. A significant change occurs between 10 $MPa^{1/2}$

and 15 $MPa^{1/2}$. Empirically, 15 out of 18 coformers with Ra(v) <10 $MPa^{1/2}$ formed eutectics (success rate: 83%). For the remaining design space, where 10 $MPa^{1/2}$ < Δδ < 23 $MPa^{1/2}$, 4 out of 9 coformers formed eutectics (success rate: 44%). For Δδ, 16 out of 18 coformers with Δδ <10 $MPa^{1/2}$ formed eutectics (success rate: 89%), while 3 out of 9 coformer formed a eutectic when 10 $MPa^{1/2}$ < Δδ < 21 $MPa^{1/2}$ (success rate: 33%).

CONCLUSIONS

A pool of 71 coformers candidates were reduced to a more feasible and representative subset of 27 coformers using Hansen Solubility Parameters δTotal and one-way ANOVA. Following co-grinding of 1:1 stoichiometric ratio's, melting endotherms and enthalpy changes could be measured using DSC and characterized for evidence of interactions including eutectic formation. A method to convert the enthalpy changes into binary scores of interaction vs. non-interaction and more specfically, eutectic vs. non-eutectic formation appears feasible. The approach enables binary fitted line analyses and logistical regression treatment of the data for a series of solubility parameter-based continuous variables based on HSPiP software Y-MB and Van Krevelen estimation methodologies. From binary fitted line analyses, confirmed interactions, not otherwise considered eutectic formation, appear to correlate more closely with Y-MB values as determined by the significantly higher R^2 (adj) values for δ(δTotal (75%), Δδ-Y-MB (72%) and Ra(v)-Y-MB (78%) with probabilities of interaction occurring when distances are <8 $MPa^{1/2}$, <17 $MPa^{1/2}$, and < 17$MPa^{1/2}$, respectively. By comparison, the use of Van Krevelen-based parameters for Ra(v) and Δδ displayed lower correlation between the parameters and the findings of interaction vs. non-interaction, with R^2 (adj) values of 28% and 36%, respectively. Using logistical regression, statistically significant relationships were determined for Y-MB derived independent continuous variables δ(δTotal), Δδ-Y-MB, Ra(v)-Y-MB, hydrogen bond/donor/acceptor (δ(δH), δ(δHD), δ(δHA)) and eutectic formation. Similarly, statistically significant relationships were also found for the Van Krevelen derived parameters, Ra(v), Δδ and eutectic formation. Regardless of the derived parameters, all models reinforce the expected relationships between these parameters and observations of miscibility as exemplified through eutectic formation. Logistic regression and logit function determinations of log odds estimates enabled calculations of predicted probabilities and may accelerate future supplementary coformer screening. Despite the small data set and limitations, overall predicted vs actual success rates are high and support the use of HSP as an in silico interaction/eutectic screening tool. This tool may improve experimental efficiency and effectiveness through a reduction in the extent of preliminary experimentation.

ACKNOWLEDGMENTS

The authors wish to thank AMO Pharma Ltd for the donation of tideglusib DS for this research, and Dr. Pardeep Gupta, Dr Jasmin Monpara and Mr. Buu Tu of the Industrial Pharmacy Laboratory (IPHL) at USciences for the use of the TA Instruments Discovery DSC 2500 series. This work was supported by the Jacob Gelb Fellowship for academic excellence.

REFERENCES.

1) Amidon, G. L., et al. (1995). "A theoretical basis for a biopharmaceutic drug classification: the correlation of in vitro drug product dissolution and in vivo bioavailability." Pharmaceutical research 12(3): 413-420.
2) Anagnostou, E., et al. (2018). A Phase 2 Randomized, Placebo-Controlled Trial of Tideglusib, an Orally Administered GSK-3 Beta Inhibitor, in the Treatment of Adolescents With ASD. 65th Annual Meeting, AACAP.
3) Araya-Sibaja, A. M., et al. (2019). "Drug Solubility Enhancement through the Preparation of Multicomponent Organic Materials: Eutectics of Lovastatin with

Carboxylic Acids." Pharmaceutics 11(3): 112.

4) Bagley, E., et al. (1971). "Three-dimensional solubility parameters and their relationship to internal pressure measurements in polar and hydrogen bonding solvents." Journal of paint technology 43(555): 35-42.
5) Bank, H. S. D. (2018). " PubChem Annotation Record for Malonic acid." National Center for Biotechnology Information.
6) Bora, P., et al. (2018). "Regulation of π⋯ π Stacking Interactions in Small Molecule Cocrystals and/or Salts for Physiochemical Property Modulation." 18(3): 1448-1458.
7) Bradley, R. and T. Cleasby (1953). "346. The vapour pressure and lattice energy of hydrogen-bonded crystals. Part I. Oxamide, oxamic acid, and rubeanic acid." Journal of the Chemical Society (Resumed): 1681-1684.
8) Chadha, K., et al. (2017). "Is Failure of cocrystallization actually a failure? Eutectic formation in cocrystal screening of hesperetin." Journal of pharmaceutical sciences 106(8): 2026-2036.
9) Charman, S. A., et al. (1992). "Self-emulsifying drug delivery systems: formulation and biopharmaceutic evaluation of an investigational lipophilic compound." Pharmaceutical research 9(1): 87-93.
10) Charman, W. N., et al. (1997). "Physicochemical and physiological mechanisms for the effects of food on drug absorption: the role of lipids and pH." Journal of pharmaceutical sciences 86(3): 269-282.
11) Cherukuvada, S. and T. N. Guru Row (2014). "Comprehending the formation of eutectics and cocrystals in terms of design and their structural interrelationships." Crystal growth & design 14(8): 4187-4198.
12) Cruz-Cabeza, A. J., et al. (2019). "Polymorphism in p-aminobenzoic acid." CrystEngComm 21(13): 2034-2042.
13) Dai, X.-L., et al. (2019). "Intermolecular interactions and permeability of 5-fluorouracil cocrystals with a series of isomeric hydroxybenzoic acids: a combined theoretical and experimental study." CrystEngComm 21(34): 5095-5105.
14) Fábián, L. (2009). "Cambridge structural database analysis of molecular complementarity in cocrystals." Crystal growth and design 9(3): 1436-1443.
15) Ferloni, P. and G. Della Gatta (1995). "Heat capacities of urea, N-methylurea, N-ethylurea, N-(n) propylurea, and N-(n) butylurea in the range 200 to 360 K." Thermochimica acta 266: 203-212.
16) Fischer, F., et al. (2015). "Synthesis, structure determination, and formation of a theobromine: oxalic acid 2: 1 cocrystal." CrystEngComm 17(4): 824-829.
17) Greenhalgh, D. J., et al. (1999). "Solubility parameters as predictors of miscibility in solid dispersions." Journal of pharmaceutical sciences 88(11): 1182-1190.
18) Gu, C.-H., et al. (2007). "Predicting effect of food on extent of drug absorption based on physicochemical properties." Pharmaceutical research 24(6): 1118-1130.
19) Hansen, C. M. (1967). "The three dimensional solubility parameter." Danish Technical: Copenhagen 14.
20) Hino, T., et al. (2001). "Assessment of nicotinamide polymorphs by differential scanning calorimetry." Thermochimica acta 374(1): 85-92.
21) Holm, R., et al. (2003). "Examination of oral absorption and lymphatic transport of halofantrine in a triple-cannulated canine model after administration in self-microemulsifying drug delivery systems (SMEDDS) containing structured triglycerides." European Journal of Pharmaceutical Sciences 20(1): 91-97.
22) Horrigan, J., et al. (2020). "A phase 2 study of AMO-02 (Tideglusib) in congenital and childhood-onset myotonic dystrophy type 1 (DM1)." Pediatric Neurology 112: 84-93.

23) Horrigan, J., et al. (2018). "AMO-02 (tideglusib) for the treatment of congenital and childhood onset myotonic dystrophy type 1." 28: S14.
24) Hoy, K. (1985). "Tables of Solubility Parameters, Solvent and Coatings Materials Research and Development Department, Union Carbide Corporation." J Paint Techn (1970) 42: 76.
25) Joel H. Hildebrand, R. L. S. (1950). "The Solubility of Nonelectrolytes." New York: Reinhold Publishing Corporation(3rd Edition): 488 pp.
26) Karagianni, A., et al. (2018). "Pharmaceutical cocrystals: New solid phase modification approaches for the formulation of APIs." 10(1): 18.
27) Krevelen, D. W. v., K Te Nijenhuis (2009). "Properties of Polymers : Their Correlation with Chemical Structure; Their Numerical Estimation and Prediction from Additive Group." Elsevier Science & Technology: 219.
28) Lipinski, C. A. (2000). "Drug-like properties and the causes of poor solubility and poor permeability." Journal of pharmacological and toxicological methods 44(1): 235-249.
29) Lipinski, C. A. (2003). Physicochemical properties and the discovery of orally active drugs: technical and people issues. Molecular informatics: confronting complexity, proceedings of the Beilstein-Institut Workshop (Frankfurt, Germany).
30) Lovestone, S., et al. "ARGO investigators (2015) A phase II trial of tideglusib in Alzheimer's disease." 45: 75-88.
31) Lu, E., et al. (2008). "A rapid thermal method for cocrystal screening." CrystEngComm 10(6): 665-668.
32) Mohammad, M. A., et al. (2011). "Hansen solubility parameter as a tool to predict cocrystal formation." International journal of pharmaceutics 407(1-2): 63-71.
33) Nagy, S., et al. (2019). "Reliability of the Hansen solubility parameters as co-crystal formation prediction tool." International journal of pharmaceutics 558: 319-327.
34) Nehm, S. J., et al. (2006). "Phase solubility diagrams of cocrystals are explained by solubility product and solution complexation." Crystal growth & design 6(2): 592-600.
35) Panzade, P., et al. (2017). "Pharmaceutical Cocrystal of Piroxicam: Design, Formulation and Evaluation." 7(3): 399.
36) Raman, S. and J. E. Polli (2016). "Prediction of positive food effect: Bioavailability enhancement of BCS class II drugs." International journal of pharmaceutics 506(1-2): 110-115.
37) Roca-Paixão, L., et al. (2019). "Affinity prediction computations and mechanosynthesis of carbamazepine based cocrystals." CrystEngComm 21(45): 6991-7001.
38) Rosbottom, I., et al. (2018). "Conformational and structural stability of the single molecule and hydrogen bonded clusters of para aminobenzoic acid in the gas and solution phases." CrystEngComm 20(46): 7543-7555.
39) Saganowska, P. and M. Wesolowski (2018). "DSC as a screening tool for rapid co-crystal detection in binary mixtures of benzodiazepines with co-formers." Journal of Thermal Analysis and Calorimetry 133(1): 785-795.
40) Schultheiss, N. and A. Newman (2009). "Pharmaceutical cocrystals and their physicochemical properties." Crystal growth and design 9(6): 2950-2967.
41) Surov, A. O., et al. (2017). "Cocrystal formation, crystal structure, solubility and permeability studies for novel 1, 2, 4-thiadiazole derivative as a potent neuroprotector." European Journal of Pharmaceutical Sciences 109: 31-39.
42) Tolosa, E., et al. "Investigators T (2014) A phase 2 trial of the GSK-3 inhibitor tideglusib in progressive supranuclear palsy." 29(4): 470-478.
43) Van Krevelen, D. and K. Te Nijenhuis (1990). "Polymer properties." Prop. Polym 3: 3-5.

44) Wicker, J. G., et al. (2017). "Will they co-crystallize?" CrystEngComm 19(36): 5336-5340.

45) Zhang, S.-W., et al. (2017). "Celecoxib–nicotinamide cocrystal revisited: can entropy control cocrystal formation?" Crystal growth & design 17(5): 2836-2843.

How to cite this article:

Bernard Kiernan, Sriramakamal Jonnalagadda , Mike Snape ***Complementarity Of Differential Scanning Calorimetry-Measured (DSC) Enthalpy Changes With The Hansen Solubility Parameters In Silico Prediction For Miscibility And Eutectic Screening For The Gsk-3β Inhibitor, Tideglusib And 27 Coformer Candidates*** **Br J Bio Med Res , Vol.05, Issue 04, Pg.1749 - 1780, July - August 2021. ISSN:2456-9739 Cross Ref DOI : https://doi.org/10.24942/bjbmr.2021.845**

Source of Support: Nil **Conflict of Interest:** None